

# OUT OF EQUILIBRIUM DYNAMICS OF AN INFLATIONARY PHASE TRANSITION

**D. Boyanovsky<sup>(a)</sup>, D. Cormier<sup>(b)</sup>, H. J. de Vega<sup>(c)</sup>, and R. Holman<sup>(b)</sup>**

*(a) Department of Physics and Astronomy, University of Pittsburgh, Pittsburgh, PA. 15260,  
U.S.A.*

*(b) Department of Physics, Carnegie Mellon University, Pittsburgh, PA. 15213, U. S. A.*

*(c) Laboratoire de Physique Théorique et Hautes Energies, Université Pierre et Marie Curie  
(Paris VI), Tour 16, 1er. étage, 4, Place Jussieu 75252 Paris cedex 05, France  
(October 1996)*

## Abstract

We study the non-linear dynamics of an inflationary phase transition in a quartically self coupled inflaton model within the framework of a de Sitter background. Large  $N$  and Hartree non-perturbative approximations combined with non-equilibrium field theory methods are used to study the self-consistent time evolution including backreaction effects. We find that when the system cools down from an initial temperature  $T_i > T_c$  to below  $T_c$  with the initial value of the zero mode of the inflaton  $\phi(0) \ll m\lambda^{-1/4}$ , the dynamics is determined by the growth of long-wavelength quantum fluctuations. For  $\phi(0) \gg m\lambda^{-1/4}$  the dynamics is determined by the evolution of the classical zero mode. In the regime where spinodal quantum fluctuations give the most important contribution to the non-equilibrium dynamics, we find that they modify the equation of state providing a graceful exit from the inflationary stage. Inflation ends through this new mechanism at a time scale  $t_s \geq [H/m^2] \ln [\lambda^{-1}]$  which for  $H \geq m$  and very weak coupling allows over one hundred e-folds during the de Sitter phase. Spatially correlated domains grow to be of horizon-size and quantum fluctuations “freeze-out” for times  $t > t_s$ .

## I. INTRODUCTION

For all of its observational success, the standard big bang cosmology is not without its shortcomings. The inflationary scenario was conceived [1] to overcome many of these shortcomings, chief amongst them the flatness and horizon problems. The original old inflationary scenario [1] required a first-order phase transition with strong supercooling, during which the scale factor grew exponentially thus solving the homogeneity and flatness problem. This model, however, lacked any mechanism to provide a successful exit from the inflationary phase [2]. The new inflationary or ‘slow-rollover’ scenario [3,4] overcame these problems. In these scenarios, a phase transition from an unbroken phase to a symmetry broken one takes place, and the scalar field, whose expectation value serves as the order parameter, drives inflation. This scalar field, the inflaton, drives a stage of exponential (de Sitter) expansion while it slowly rolls down the potential hill. Other versions, such as chaotic inflation [5] in which a phase transition is not necessary have been advocated (for reviews of inflationary cosmology, see [6–9]).

Phase transitions play an important role in the early universe, and, as mentioned above, are pivotal to many inflationary models. They are also necessary in models in which topological defects provide the seeds for density perturbations [10]. It has been pointed out by many authors that using flat space-time effective potentials and equilibrium concepts to describe the dynamics of the inflationary phase transition can be misleading. Both gravitational effects as well as those due to quantum and thermal fluctuations have been studied and found to be very important for the description of the dynamics [11–16].

Although there have been previous studies of the dynamics of phase transitions [14–16], most of the attempts were hampered by the lack of a self-consistent non-perturbative treatment of the non-linearities and backreaction effects. It is only recently that non-equilibrium methods have been developed to study real time phenomena during phase transitions [17–20] and other strongly out of equilibrium situations [21], including non-perturbative treatments [22–24]. During the last few years these methods have been adapted to study strongly out of equilibrium phenomena in cosmology, allowing the understanding of the dynamics of non-linear field theory in such situations [25,26].

Studies of the dynamics of typical second order phase transitions in Minkowski space-time have revealed a wealth of new and interesting phenomena. In situations in which the phase transition occurs on time scales which are faster than the relaxation time of long-wavelength fluctuations, the dynamics is driven by the growth of long-wavelength, spinodal instabilities. The backreaction of these quantum and thermal fluctuations dramatically modifies

the evolution of the zero mode of the scalar field eventually shutting off the instabilities [27–29]. These instabilities are the hallmark of the phase transition and are responsible for the formation and growth of correlated domains [28,29].

The nature of these instabilities and their intrinsic non-perturbative dynamics is rather simple to understand [27–29]. As the system cools down from a quasi-equilibrium disordered high temperature phase to below the critical temperature the effective mass of the scalar field becomes negative. If the expectation value of the field was zero in the equilibrium high temperature phase, it will remain zero below the critical temperature in the absence of biasing fields. The fluctuations of the field will grow in time and eventually become large enough to sample the minima of the (effective) potential, which are non-perturbatively large in amplitude. This growth of fluctuations translates into a growth of spatial correlations of the field, resulting in domains [28]. In Minkowski space-time there is no restriction to the final size of these domains, and generically in weakly coupled theories these correlated regions reach sizes several times larger than the zero temperature correlation length [28]. In a de Sitter spacetime or in a general FRW cosmology, for that matter, causality limits the physical distance within which the order parameter can be correlated; in a de Sitter spacetime, this distance is  $d_H = H^{-1}$ , with  $H$  the Hubble constant.

The goal of this article is to study the full non-equilibrium dynamics of an inflationary phase transition including the backreaction effects in a simple model of a scalar field (the inflaton) with a quartic self-interaction. We use the methods of non-equilibrium field theory [17] combined with self-consistent, non-perturbative Hartree and large  $N$  approximations [21,22,25,26,29,30].

The metric is taken to be a fixed cosmological background within which we study the effects of quantum and thermal fluctuations on the evolution of the expectation value of the inflaton and the energy momentum tensor, both analytically and numerically, so as to follow the equation of state. When the temperature falls below the critical value, long-wavelength fluctuations grow exponentially as a result of the spinodal instabilities and their contribution to the equations of motion eventually become of the same order as the tree-level terms. We argue that in the very weakly coupled case,  $\lambda \approx 10^{-12}$ , the change in temperature and the effective mass occur on time scales much shorter than the time in which long-wavelength fluctuations can adjust to local thermodynamic equilibrium, and they fall out of equilibrium just as in a “quench” from the high temperature phase.

When these fluctuations are incorporated self-consistently as a backreaction in the evolution equations, we find, for slow-roll initial conditions, that the effects of these fluctuations dramatically change the dynamics. The unstable quantum fluctuations modify the equation

of state away from the vacuum dominated state required for de Sitter expansion, and for a reasonably wide range of parameters and initial conditions, these fluctuations provide a new mechanism to gracefully exit the inflationary stage within an acceptable number of e-folds. During this time, spatial correlations grow to reach horizon-size and freeze-out at larger times.

In the large  $N$  approximation, we find that the late time dynamics is summarized by a very useful sum rule relating the infinite time limit of the order parameter  $\phi(\infty)$  and the infinite time limit of the quantum fluctuations  $\langle\psi^2(\infty)\rangle$  as follows,

$$-|m^2| + \phi^2(\infty) + \langle\psi^2(\infty)\rangle = 0 .$$

This result implies that the excitations are massless and minimally coupled. However we find the new result that despite the fact that the relevant degrees of freedom are massless and minimally coupled asymptotically, their equal time two-point function saturates to a constant value rather than growing linearly in time.

In section II we introduce the model, the approximations, and analyze the subtle but important issues of renormalization. Section III is devoted to presenting the renormalized equations of motion and the correlation functions. Section IV and V provide an analytic and numerical study of different cases, as well as an estimate of the backreaction of the quantum fluctuations onto the scale factor. Section VI presents a discussion of the results and the final conclusions and further avenues of study.

## II. THE MODEL AND THE APPROXIMATIONS

The need for a non-perturbative treatment of nonequilibrium quantum field dynamics stems from the fact that when the temperature falls below the critical point, the effective mass term becomes negative. This results in an instability of the long-wavelength modes which grow exponentially for early times after the transition. The fluctuations of the scalar order parameter will grow in time to sample the broken symmetry vacua, leading to large amplitude fluctuations that can only be treated within a non-perturbative scheme.

There are two approximation schemes that have been used to study the non-equilibrium dynamics during phase transitions, each with its own advantages and disadvantages. The Hartree factorization [14,23,26,28] has the advantage that it can treat the dynamics of a scalar order parameter with discrete symmetry, while its disadvantage is that it is difficult to implement consistently beyond the lowest (mean field) level. The advantage of the large  $N$  approximation [21,22,25,26,30] is that it allows a consistent expansion in a small parameter

( $1/N$ ) and correctly treats continuous symmetries in the sense that it implements Goldstone's theorem. Moreover, the large  $N$  expansion becomes a  $\lambda/N$  expansion for small values of  $\lambda$ . Therefore, it may be a reliable approximation for the typical values of  $\lambda$  used for inflation even when  $N = 1$ . It should be noted that when spontaneous symmetry breaking is present, the large  $N$  limit always produces massless Goldstone bosons.

Both methods implement a resummation of a select set of diagrams to all orders and lead to a system of equations that is energy conserving in Minkowski space time, and as will be shown below, satisfies covariant conservation of the energy momentum tensor in FRW cosmologies. Furthermore, both methods are renormalizable and numerically implementable. Given that both methods have advantages and disadvantages and that choosing a particular scheme will undoubtedly lead to criticism and questions about their reliability, we will study *both*, comparing the results to obtain some universal features of the dynamics.

We restrict our study to a spatially flat Friedmann-Robertson-Walker universe with scale factor,  $a(t)$ , and metric,

$$ds^2 = dt^2 - a^2(t) d\vec{x}^2, \quad (2.1)$$

and focus in particular on the case of a de Sitter space-time with scale factor,

$$a(t) = e^{Ht}. \quad (2.2)$$

The action and Lagrangian density are given by,

$$S = \int d^4x \mathcal{L}, \quad (2.3)$$

$$\mathcal{L} = a^3(t) \left[ \frac{1}{2} \dot{\vec{\Phi}}^2(x) - \frac{1}{2} \frac{(\vec{\nabla} \vec{\Phi}(x))^2}{a^2(t)} - V(\vec{\Phi}(x)) \right], \quad (2.4)$$

$$V(\vec{\Phi}) = \frac{\lambda}{8N} \left( \vec{\Phi}^2 + \frac{2NM^2}{\lambda} \right)^2 ; \quad M^2 = -m^2 + \xi \mathcal{R}, \quad (2.5)$$

$$\mathcal{R} = 6 \left( \frac{\ddot{a}(t)}{a(t)} + \frac{\dot{a}^2(t)}{a^2(t)} \right), \quad (2.6)$$

where we have included the coupling of  $\Phi(x)$  to the scalar curvature  $\mathcal{R}(t)$  since it will arise as a consequence of renormalization. In the de Sitter universe (2.2),  $\mathcal{R} = 12H^2$ . The canonical momentum conjugate to  $\Phi(x)$  is,

$$\vec{\Pi}(x) = a^3(t) \dot{\vec{\Phi}}(x), \quad (2.7)$$

and the *time dependent* Hamiltonian is given by,

$$H(t) = \int d^3x \left\{ \frac{\vec{\Pi}^2(x)}{2a^3(t)} + \frac{a(t)}{2} (\nabla \vec{\Phi}(x))^2 + a^3(t) V(\vec{\Phi}) \right\}. \quad (2.8)$$

### A. The Hartree Approximation

To implement the Hartree approximation, we set  $N = 1$  and write,

$$\Phi(\vec{x}, t) = \phi(t) + \psi(\vec{x}, t), \quad (2.9)$$

with,

$$\phi(t) = \langle \Phi(\vec{x}, t) \rangle; \quad \langle \psi(\vec{x}, t) \rangle = 0, \quad (2.10)$$

where the expectation value is defined by the non-equilibrium density matrix specified below, and we have assumed spatial translational invariance, compatible with a spatially flat metric. The Hartree approximation is obtained after the factorization,

$$\psi^3(\vec{x}, t) \rightarrow 3\langle \psi^2(\vec{x}, t) \rangle \psi(\vec{x}, t), \quad (2.11)$$

$$\psi^4(\vec{x}, t) \rightarrow 6\langle \psi^2(\vec{x}, t) \rangle \psi^2(\vec{x}, t) - 3\langle \psi^2(\vec{x}, t) \rangle^2, \quad (2.12)$$

where by translational invariance, the expectation values only depend on time. In this approximation, the Hamiltonian becomes quadratic at the expense of a self-consistent condition.

At this stage we must specify the non-equilibrium state in which we compute the expectation values above. In non-equilibrium field theory, the important ingredient is the time evolution of the density matrix  $\rho(t)$  (see [17] and references therein). This density matrix obeys the quantum Liouville equation whose solution only requires an initial condition  $\rho(t_i)$  [17,19,20,25,26]. The choice of initial conditions for this density matrix is an issue that pervades any calculation in cosmology. Since we want to study the dynamics of the phase transition, it is natural to consider initial conditions that describe the *instantaneous* modes of the time dependent Hamiltonian as being initially in local thermodynamic equilibrium at some temperature  $T_i > T_c$ . Given this initial density matrix, we then evolve it in time

using the time dependent Hamiltonian as in [25] or alternatively using the complex time path integral method as described in [17,19–21,26].

Following the steps of references [26–28] we find the equation of motion for the expectation value of the inflaton field to be,

$$\ddot{\phi}(t) + 3H\dot{\phi}(t) + M^2\phi(t) + \frac{\lambda}{2}\phi^3(t) + \frac{3\lambda}{2}\phi(t)\langle\psi^2(t)\rangle = 0. \quad (2.13)$$

The equal time correlation function is obtained from the coincidence limit of the non-equilibrium Green's functions, which are obtained from the mode functions obeying

$$\left[ \frac{d^2}{dt^2} + 3H\frac{d}{dt} + \omega_k^2(t) \right] f_k(t) = 0, \quad (2.14)$$

with the effective frequencies,

$$\omega_k^2(t) = \frac{k^2}{a^2(t)} + M^2(t), \quad (2.15)$$

where

$$M^2(t) = M^2 + \frac{3\lambda}{2}\phi^2(t) + \frac{3\lambda}{2}\langle\psi^2(t)\rangle. \quad (2.16)$$

At this stage we must provide the initial conditions on the mode functions  $f_k(t)$ . As mentioned above our choice of initial conditions on the density matrix is that of local thermodynamic equilibrium for the instantaneous modes of the time dependent Hamiltonian at the initial time. Therefore we choose the initial conditions on the mode functions to represent positive energy particle states of the instantaneous Hamiltonian at  $t = 0$ , which we chose as the initial time. Therefore our choice of boundary conditions at  $t = 0$  is

$$f_k(0) = \frac{1}{\sqrt{W_k}}; \quad \dot{f}_k(0) = -i\sqrt{W_k}; \quad W_k = \sqrt{k^2 + M_0^2}, \quad (2.17)$$

where the mass  $M_0$  determines the frequencies  $\omega_k(0)$  and will be obtained explicitly later. With these boundary conditions, the mode functions  $f_k(0)$  correspond to positive frequency modes (particles) of the instantaneous quadratic Hamiltonian for oscillators of mass  $M_0$ .

The equal time correlation function is given in terms of the mode functions as [21,25,27–29],

$$\langle\psi^2(t)\rangle = \int \frac{d^3k}{(2\pi)^3} \frac{|f_k(t)|^2}{2} \coth \left[ \frac{W_k}{2T_i} \right]. \quad (2.18)$$

The energy and pressure density are given by [26],

$$\begin{aligned}\varepsilon = & \frac{1}{2}\dot{\phi}^2(t) + \frac{\lambda}{8} \left( \phi^2(t) + \frac{2M^2}{\lambda} \right)^2 + \\ & \frac{1}{2} \int \frac{d^3k}{2(2\pi)^3} \coth \left[ \frac{W_k}{2T_i} \right] \left[ |\dot{f}_k(t)|^2 + \omega_k^2(t) |f_k(t)|^2 \right] - \frac{3\lambda}{8} \langle \psi^2(t) \rangle^2,\end{aligned}\quad (2.19)$$

$$p + \varepsilon = \dot{\phi}^2(t) + \int \frac{d^3k}{2(2\pi)^3} \coth \left[ \frac{W_k}{2T_i} \right] \left[ |\dot{f}_k(t)|^2 + \frac{k^2}{3a^2(t)} |f_k(t)|^2 \right]. \quad (2.20)$$

It is straightforward to show using the equations of motion (2.13,2.14) that the bare energy is covariantly conserved,

$$\dot{\varepsilon} + 3H(p + \varepsilon) = 0. \quad (2.21)$$

## B. The Large $N$ Approximation

To obtain the proper large  $N$  limit, the vector field is written as,

$$\vec{\Phi}(\vec{x}, t) = (\sigma(\vec{x}, t), \vec{\pi}(\vec{x}, t)),$$

with  $\vec{\pi}$  an  $N - 1$ -plet, and we write,

$$\sigma(\vec{x}, t) = \sqrt{N}\phi(t) + \chi(\vec{x}, t) \quad ; \quad \langle \sigma(\vec{x}, t) \rangle = \sqrt{N}\phi(t) \quad ; \quad \langle \chi(\vec{x}, t) \rangle = 0. \quad (2.22)$$

To implement the large  $N$  limit in a consistent manner, one may introduce an auxiliary field as in [22,30]. However, the leading order contribution can be obtained equivalently by invoking the factorization,

$$\chi^4 \rightarrow 6\langle \chi^2 \rangle \chi^2 + \text{constant}, \quad (2.23)$$

$$\chi^3 \rightarrow 3\langle \chi^2 \rangle \chi, \quad (2.24)$$

$$(\vec{\pi} \cdot \vec{\pi})^2 \rightarrow 2\langle \vec{\pi}^2 \rangle \vec{\pi}^2 - \langle \vec{\pi}^2 \rangle^2 + \mathcal{O}(1/N), \quad (2.25)$$

$$\vec{\pi}^2 \chi^2 \rightarrow \langle \vec{\pi}^2 \rangle \chi^2 + \vec{\pi}^2 \langle \chi^2 \rangle, \quad (2.26)$$

$$\vec{\pi}^2 \chi \rightarrow \langle \vec{\pi}^2 \rangle \chi. \quad (2.27)$$

To obtain a large  $N$  limit, we define,

$$\vec{\pi}(\vec{x}, t) = \psi(\vec{x}, t) \overbrace{(1, 1, \dots, 1)}^{N-1}, \quad (2.28)$$

where the large  $N$  limit is implemented by the requirement that,



$$\langle \psi^2 \rangle \approx \mathcal{O}(1) , \langle \chi^2 \rangle \approx \mathcal{O}(1) , \phi \approx \mathcal{O}(1). \quad (2.29)$$

The leading contribution is obtained by neglecting the  $\mathcal{O}(1/N)$  terms in the formal limit. The resulting Lagrangian density is quadratic, with a linear term in  $\chi$ . The equations of motion in this case become,

$$\ddot{\phi}(t) + 3H\dot{\phi}(t) + M^2\phi(t) + \frac{\lambda}{2}\phi^3(t) + \frac{\lambda}{2}\phi(t)\langle\psi^2(t)\rangle = 0, \quad (2.30)$$

$$\langle\psi^2(t)\rangle = \int \frac{d^3k}{(2\pi)^3} \frac{|f_k(t)|^2}{2} \coth \left[ \frac{W_k}{2T_i} \right], \quad (2.31)$$

with the mode functions,

$$\left[ \frac{d^2}{dt^2} + 3H\frac{d}{dt} + \omega_k^2(t) \right] f_k(t) = 0, \quad (2.32)$$

and the effective frequencies,

$$\omega_k^2(t) = \frac{k^2}{a^2(t)} + M^2(t), \quad (2.33)$$

where,

$$M^2(t) = M^2 + \frac{\lambda}{2}\phi^2(t) + \frac{\lambda}{2}\langle\psi^2(t)\rangle. \quad (2.34)$$

The initial conditions are chosen to reflect the same physical situation as in the Hartree case, that is, the instantaneous particle states of the Hamiltonian at  $t = 0$  are in local thermodynamic equilibrium at some initial temperature higher than the critical value. Thus, as in the Hartree case but with modified frequencies, the initial conditions at  $t = 0$  are chosen to describe the instantaneous positive energy states,

$$f_k(0) = \frac{1}{\sqrt{W_k}}; \dot{f}_k(0) = -i\sqrt{W_k}; W_k = \sqrt{k^2 + M_0^2}. \quad (2.35)$$

We have maintained the same names for the mode functions and  $M_0$  to avoid cluttering of notation; their meaning for each case should be clear from the context. Notice that the difference between the Hartree and large  $N$  case is rather minor. The most significant difference is that, in the equations for the zero modes, the Hartree case displays a factor 3 difference between the tree level non-linear term and the contribution from the fluctuation as compared to the corresponding terms in the large  $N$  case. The equations for the mode functions are the same upon a trivial rescaling of the coupling constant by a factor 3.

The particular case with  $\phi(t) = 0$  is of interest, since by symmetry, it is a fixed point of the dynamics of the zero mode and corresponds to the case in which the phase transition

occurs from the symmetric phase into the broken phase in the absence of symmetry breaking perturbations or initial bias in the field. In this important case, the Hartree and large  $N$  mode equations are identical after the coupling constant is rescaled by a factor of 3, and our conclusions will be *universal* in the sense that both the large  $N$  approximation and the Hartree approximation describe the same non-perturbative dynamics. In the large  $N$  limit we find the energy density to be given by,

$$\begin{aligned} \frac{\varepsilon}{N} = & \frac{1}{2} \dot{\phi}^2(t) + \frac{\lambda}{8} \left( \phi^2(t) + \frac{2M^2}{\lambda} \right)^2 + \\ & \frac{1}{2} \int \frac{d^3k}{2(2\pi)^3} \coth \left[ \frac{W_k}{2T_i} \right] \left[ |\dot{f}_k(t)|^2 + \omega_k^2(t) |f_k(t)|^2 \right] - \frac{\lambda}{8} \langle \psi^2(t) \rangle^2, \end{aligned} \quad (2.36)$$

and  $(p + \varepsilon)/N$  has the same form as for the Hartree case above (eq. (2.20)), but in terms of the mode functions obeying the large  $N$  equations. Again, it is straightforward to show that the bare energy is covariantly conserved by using the equations of motion for the zero mode and the mode functions. Note that equation (2.21) also holds in the large  $N$  limit.

A relation analogous to (2.21) holds for the integrands of  $\varepsilon$  and  $\varepsilon + p$  in eqs.(2.19) and (2.20). Namely,

$$\dot{\varepsilon}_k(t) + 3H\sigma_k(t) = \frac{d}{dt}[M^2(t)] |f_k(t)|^2. \quad (2.37)$$

Here,

$$\begin{aligned} \varepsilon_k(t) = & |\dot{f}_k(t)|^2 + \omega_k^2(t) |f_k(t)|^2, \\ \sigma_k(t) = & 2 \left[ |\dot{f}_k(t)|^2 + \frac{k^2}{3a^2(t)} |f_k(t)|^2 \right]. \end{aligned} \quad (2.38)$$

Equation (2.37) will be used below to prove that the renormalized energy is conserved.

### III. RENORMALIZED EQUATIONS OF MOTION

Renormalization is a very subtle but important issue in gravitational backgrounds [13,32,33]. The fluctuation contribution  $\langle \psi^2(\vec{x}, t) \rangle$ , the energy and the pressure all need to be renormalized. The renormalization aspects in curved space times have been discussed at length in the literature [13,32,33] and has been extended to the Hartree and large  $N$  self-consistent approximations for the non-equilibrium backreaction problem in [25,30].

In terms of the effective mass term for the large  $N$  limit given by (2.34) and the Hartree case, eq. (2.16), and defining the quantity,

$$B(t) \equiv a^2(t) \left( M^2(t) - \mathcal{R}/6 \right), \quad (3.1)$$

we find the following large  $k$  behavior for the case of an *arbitrary* scale factor  $a(t)$  (with  $a(0) = 1$ ),

$$\begin{aligned} |f_k(t)|^2 &= \frac{1}{ka^2(t)} + \frac{1}{2k^3a^2(t)} \left[ H^2(0) - B(t) \right] \\ &\quad + \frac{1}{8a(t)^2 k^5} \left\{ B(t)[3B(t) - 2H^2(0)] + a(t) \frac{d}{dt} [a(t)\dot{B}(t)] + D_0 \right\} + \mathcal{O}(1/k^7) \\ |\dot{f}_k(t)|^2 &= \frac{k}{a^4(t)} + \frac{1}{ka^2(t)} \left[ H^2(t) + \frac{H^2(0)}{2a^2(t)} + \frac{1}{2} \left( M^2(t) - \mathcal{R}/6 \right) \right] \\ &\quad + \frac{1}{8a(t)^4 k^3} \left\{ -B(t)^2 - a(t)^2 \ddot{B}(t) + 3a(t)\dot{a}(t)\dot{B}(t) - 4\dot{a}^2(t)B(t) \right. \\ &\quad \left. + 2H^2(0)[2\dot{a}^2(t) + B(t)] + D_0 \right\} + \mathcal{O}(1/k^5). \end{aligned} \quad (3.2)$$

The constant  $D_0$  depends on the initial conditions and is unimportant for our analysis.

Although the divergences can be dealt with by dimensional regularization, this procedure is not well suited to numerical analysis. We will make our subtractions using an ultraviolet cutoff constant in *physical coordinates*. This guarantees that the counterterms will be time independent. The renormalization then proceeds much in the same manner as in reference [25]; the quadratic divergences renormalize the mass and the logarithmic terms renormalize coupling constant and the coupling to the Ricci scalar. The logarithmic subtractions can be neglected because of the coupling  $\lambda \approx 10^{-12}$ . Using the Planck scale as the cutoff and the inflaton mass  $m_R$  as a renormalization point, these terms are of order  $\lambda \ln[M_{pl}/m_R] \leq 10^{-10}$ , for  $m \geq 10^9 \text{GeV}$ . An equivalent statement is that for these values of the coupling and inflaton masses, the Landau pole is beyond the physical cutoff  $M_{pl}$ . Our relative error in the numerical analysis is of order  $10^{-8}$ , therefore our numerical study is insensitive to the logarithmic corrections. Though these corrections are fundamentally important, numerically they can be neglected. Therefore, in what follows, we will neglect logarithmic renormalization and subtract only quartic and quadratic divergences in the energy and pressure, and quadratic divergences in the fluctuation contribution.

Using the large  $k$  behavior of the mode functions, we find the finite temperature factor to be [25],

$$\int d^3k \frac{|f_k(t)|^2}{\exp[\frac{W_k}{T_i}] - 1} = \frac{1}{24} \left[ \frac{T_i^2}{a^2(t)} \right] [1 + \mathcal{O}(M_0/T_i) + \mathcal{O}(\ln(M_0/T_i)) + \dots], \quad (3.3)$$

where we have used  $T_i > T_c \gg M_0$ . The first term in (3.3) arises from the  $1/[ka^2(t)]$  in the asymptotic limit (3.2). For the large  $N$  case, we find the renormalization condition,

$$-m_B^2 + \frac{\lambda_B}{2}\phi^2(t) + \xi_B \mathcal{R} + \frac{\lambda_B}{2}\langle\psi^2(t)\rangle_B = m_R^2(t, T_i) + \frac{\lambda_R}{2}\phi^2(t) + \xi_R \mathcal{R} + \frac{\lambda_R}{2}\langle\psi^2(t)\rangle_R, \quad (3.4)$$

with the effective time dependent mass term in de Sitter space time, and subtracted fluctuation contribution [25],

$$m_R^2(t, T_i) = m_R^2 \left[ \frac{T_i^2}{T_c^2} e^{-2Ht} - 1 \right], \quad \langle\psi^2(t)\rangle_R = \frac{1}{4\pi^2} \int_0^\infty k^2 dk \coth \left[ \frac{W_k}{2T_i} \right] \left\{ |f_k(t)|^2 - \frac{1}{ka^2(t)} - \frac{\theta(k - \kappa)}{2k^3 a^2(t)} \left[ H^2(0) - a^2(t) (M^2(t) - \mathcal{R}/6) \right] \right\}, \quad (3.5)$$

where  $\kappa$  is a renormalization point, which for convenience will be chosen as  $\kappa = |m_R|$ , i.e. the renormalized inflaton mass. The Hartree case is similar but with a rescaling of the coupling constant by a factor 3. We will fix the renormalized coupling to the Ricci scalar to be  $\xi_R = 0$ , thus ensuring minimal coupling in the renormalized theory.

Assuming that  $T_i/T_c \approx \mathcal{O}(1)$ , we see that the phase transition occurs within the first few e-folds of inflation. When the temperature falls below the critical value, the effective mass becomes negative. As will be seen explicitly below, when this occurs, long-wavelength modes become unstable and grow. Local thermodynamic equilibrium will set in again if the contribution from the quantum fluctuations can grow and adjust to compensate for the negative mass terms on the same time scales as that in which the temperature drops. However, as discussed below, for very weak coupling the important time scales for the non-equilibrium fluctuations are of the order of  $[H/m_R^2] \ln[1/\lambda]$ , which are much longer than the time it takes for the temperature to drop well below the critical value to practically zero. Thus, the non-equilibrium dynamics will proceed as if the phase transition occurred via a “quench”, that is with an effective mass term,

$$m_{eff}^2(t) = m_i^2 \theta(t_i - t) - m_R^2 \theta(t - t_i) \quad ; \quad m_i^2 = m_R^2 \left[ \frac{T_i^2}{T_c^2} - 1 \right] > 0. \quad (3.6)$$

Therefore we choose the initial conditions on the mode functions at  $t_i = 0$  to be given in terms of the effective mass,

$$M_0^2 = m_R^2 \left[ \frac{T_i^2}{T_c^2} - 1 \right] + \frac{\lambda_R}{2} \phi^2(0) \quad ; \quad \frac{T_i}{T_c} > 1, \quad (3.7)$$

with  $\lambda_R \rightarrow 3\lambda_R$  for the Hartree case.

We introduce the following dimensionless quantities and definitions,

$$\tau = m_R t \quad ; \quad h = \frac{H}{m_R} \quad ; \quad q = \frac{k}{m_R}, \quad (3.8)$$

$$r = \frac{T_i}{T_c} \quad ; \quad \mathcal{T} = \frac{T_i}{m_R} \quad ; \quad \omega_q = \frac{W_k}{m_R} \quad ; \quad g = \frac{\lambda}{8\pi^2} , \quad (3.9)$$

$$\eta^2(\tau) = \frac{\lambda}{2m_R^2} \phi^2(t) \quad ; \quad g\Sigma(\tau) = \frac{\lambda}{2m_R^2} \langle \psi^2(t) \rangle_R , \quad (3.10)$$

$$f_q(\tau) \equiv \sqrt{m_R} f_k(t) \quad ; \quad K = \frac{\kappa}{m_R} . \quad (3.11)$$

With  $\xi_R = 0$  and  $K = 1$  the equations of motion become:

**Large N:**

$$\ddot{\eta} + 3h \dot{\eta} - \eta + \eta^3 + g\Sigma(\tau)\eta = 0 \quad (3.12)$$

$$\left[ \frac{d^2}{d\tau^2} + 3h \frac{d}{d\tau} + \frac{q^2}{a^2(\tau)} - 1 + \eta^2 + g\Sigma(\tau) \right] f_q(\tau) = 0 \quad (3.13)$$

$$f_q(0) = \frac{1}{\sqrt{\omega_q}} \quad ; \quad \dot{f}_q(0) = -i\sqrt{\omega_q} \quad ; \quad \omega_q = \sqrt{q^2 + r^2 - 1 + \eta^2(0)} \quad (3.14)$$

**Hartree:**

$$\ddot{\eta} + 3h \dot{\eta} - \eta + \eta^3 + 3g\Sigma(\tau)\eta = 0 \quad (3.15)$$

$$\left[ \frac{d^2}{d\tau^2} + 3h \frac{d}{d\tau} + \frac{q^2}{a^2(\tau)} - 1 + 3\eta^2 + 3g\Sigma(\tau) \right] f_q(\tau) = 0 \quad (3.16)$$

$$f_q(0) = \frac{1}{\sqrt{\omega_q}} \quad ; \quad \dot{f}_q(0) = -i\sqrt{\omega_q} \quad ; \quad \omega_q = \sqrt{q^2 + r^2 - 1 + 3\eta^2(0)} \quad (3.17)$$

The dots stand for derivatives with respect to  $\tau$ , and in both cases,

$$g\Sigma(\tau) = \int_0^\infty q^2 dq \coth \left[ \frac{\omega_q}{2\mathcal{T}} \right] \left\{ |f_q(\tau)|^2 - \frac{\theta(q-1)}{2q^3 a^2(t)} \left[ h^2(0) - \frac{a^2(t)}{m_R^2} (M^2(t) - \mathcal{R}/6) \right] \right\} . \quad (3.18)$$

Numerically, the most significant contribution to  $\langle \psi^2 \rangle$  arises from low wavevectors  $q \leq 10 - 20$  in all of the cases studied (see figures 1.e and 1.f below). Since  $T_i > T_c = \sqrt{24m_R^2/\lambda}$ ,  $q \ll \mathcal{T}$  and  $M_0 \ll T_i$  for these low momentum modes, they are “classical” and we can approximate,

$$\coth \left[ \frac{\omega_q}{2\mathcal{T}} \right] \approx \frac{2\mathcal{T}}{\omega_q} = \frac{2r}{\omega_q} \sqrt{\frac{24}{\lambda}} . \quad (3.19)$$

In this approximation, the fluctuation contribution becomes,

$$g\Sigma(\tau) = \bar{g} \int \frac{q^2 dq}{\omega_q} \left\{ |f_q(\tau)|^2 - \frac{\theta(q-1)}{2q^3 a^2(t)} \left[ h^2(0) - \frac{a^2(t)}{m_R^2} (M^2(t) - \mathcal{R}/6) \right] \right\},$$

$$\bar{g} = 2rg \sqrt{\frac{24}{\lambda}} = 1.103 r \sqrt{g} = 0.124 r \sqrt{\lambda}. \quad (3.20)$$

The renormalized energy density and pressure for the large  $N$  case are given by,

$$\frac{\varepsilon}{N} = \frac{2m_R^4}{\lambda} \left\{ \frac{\dot{\eta}^2}{2} + \frac{1}{4}(\eta^2 - 1)^2 + \frac{\bar{g}}{2} \int \frac{q^2 dq}{\omega_q} \left[ |\dot{f}_q(\tau)|^2 + \omega_q^2(\tau) |f_q(\tau)|^2 - \frac{2q}{a(t)^4} - \frac{\alpha(t)}{q} - \frac{\theta(q-1)}{q^3} \frac{\beta(t)}{q^3} \right] - \frac{g}{4} \Sigma(\tau) \right\}, \quad (3.21)$$

$$\frac{p + \varepsilon}{N} = \frac{2m_R^4}{\lambda} \left\{ \dot{\eta}^2 + \bar{g} \int \frac{q^2 dq}{\omega_q} \left[ |\dot{f}_q(\tau)|^2 + \frac{q^2}{3a^2(\tau)} |f_q(\tau)|^2 - \frac{4q}{3a(t)^4} - \frac{\gamma(t)}{q} - \frac{\theta(q-1)}{q^3} \delta(t) \right] \right\}, \quad (3.22)$$

with,

$$\omega_q^2(\tau) = \frac{q^2}{a^2(\tau)} - 1 + \eta^2(\tau) + g\Sigma(\tau). \quad (3.23)$$

and  $B(t)$  is given by eq.(3.1). The coefficients  $\alpha(t)$ ,  $\beta(t)$ ,  $\gamma(t)$  and  $\delta(t)$  are obtained from the asymptotic behaviour of  $\varepsilon_k(t)$  and  $\sigma_k(t)$  (2.38-3.2). We find,

$$\alpha(t) = \frac{1}{m_R^2 a(t)^4} \left[ \dot{a}^2(t) + a^2(t) M(t)^2 + H(0)^2 \right],$$

$$\beta(t) = \frac{1}{4m_R^4 a(t)^4} \left\{ B^2(t) + 2a(t)\dot{a}(t)\dot{B}(t) - 2[\dot{a}^2(t) + a^2(t) M(t)^2][B(t) - H(0)^2] + D_0 \right\},$$

$$\gamma(t) = \frac{1}{3m_R^2 a(t)^4} \left[ B(t) + 3\dot{a}^2(t) + 2H(0)^2 \right], \quad (3.24)$$

$$\delta(t) = -\frac{1}{12m_R^4 a(t)^4} \left\{ a^2(t) \ddot{B}(t) - 5a(t)\dot{a}(t)\dot{B}(t) + 6\dot{a}^2(t)[B(t) - H(0)^2] - 2H(0)^2 B(t) - 2D_0 \right\}.$$

For the Hartree case (setting  $N = 1$ ) the only changes are that we take  $g\Sigma/4 \rightarrow 3g\Sigma/4$  in the last term in the energy, and use the frequencies,

$$\omega_q^2(\tau) = \frac{q^2}{a^2(\tau)} - 1 + 3\eta^2(\tau) + 3g\Sigma(\tau), \quad (3.25)$$

and that the initial conditions on the mode functions are given by (3.17).

In order to prove that the renormalized energy and pressure fullfils the continuity equation (2.21), we need to study the properties of the subtracted terms in equations (3.21)-(3.22). Inserting the asymptotic behaviour of  $\varepsilon_k(t)$ ,  $\sigma_k(t)$  and  $|f_k(\tau)|^2$  for large  $k$  in (2.37), we find,

$$\begin{aligned} \dot{\alpha}(t) + 6H \gamma(t) &= \frac{1}{a^2(t)} \frac{d}{dt}[M^2(t)] , \\ \dot{\beta}(t) + 6H \delta(t) &= \frac{1}{2a^2(t)} [H(0)^2 - B(t)] \frac{d}{dt}[M^2(t)] . \end{aligned} \quad (3.26)$$

Using these relations and (2.37), it is straightforward to show that the renormalized energy and pressure given by eqs. (3.21)-(3.22) satisfy the continuity equation,

$$\dot{\varepsilon} + 3H(p + \varepsilon) = 0 .$$

A noteworthy point is that when the cutoff is kept fixed in *physical* coordinates, upon taking the time derivative in the integrals, there is a contribution from the upper limit of the integrals. However the subtractions guarantee that in the formal limit when the cutoff is taken to infinity this contribution vanishes. While the existence of the Landau pole beyond the Planck mass restricts taking the cutoff to infinity in this effective theory, we find that any contributions from the upper limit are numerically small. In our numerical evolution, the energy density is covariantly conserved to one part in  $10^7$ .

From the evolution of the mode functions that determine the quantum fluctuations, we can study the growth of correlated domains with the equal time correlation function,

$$\begin{aligned} S(\vec{x}, t) &= \langle \psi(\vec{x}, t) \psi(\vec{0}, t) \rangle, \\ &= \int \frac{d^3k}{(2\pi)^3} e^{i\vec{k}\cdot\vec{x}} \frac{|f_k(t)|^2}{2} \coth\left(\frac{W_k}{2T_i}\right), \end{aligned} \quad (3.27)$$

which can be written in terms of the power spectrum of quantum fluctuations,

$$\mathcal{S}(k, t) = \frac{\mathcal{S}(q, \tau)}{m_R} \quad ; \quad \mathcal{S}(q, \tau) = |f_q(\tau)|^2 \coth\left(\frac{\omega_q}{2\mathcal{T}}\right). \quad (3.28)$$

It is convenient to define the dimensionless correlation function,

$$\mathcal{S}(\rho, \tau) = \frac{S(|\vec{x}|, t)}{m_R^2} = \frac{1}{4\pi^2\rho} \int q dq \sin[q\rho] \mathcal{S}(q, \tau) ; \rho = m_R |\vec{x}|. \quad (3.29)$$

We now have all the ingredients to study the particular cases of interest.

## IV. EVOLUTION FOR $\phi(0) = \dot{\phi}(0) = 0$

### A. Analytical Results

We begin by considering the situation in which the expectation value of the inflaton field sits atop the potential hill with zero initial velocity. This situation is expected to arise if the system is initially in local thermodynamic equilibrium at an initial temperature larger than the critical temperature and cools down through the critical temperature in the absence of an external field or bias.

The order parameter and its time derivative vanish in the local equilibrium high temperature phase, and this condition is a fixed point of the evolution equation for the zero mode of the inflaton. There is no rolling of the inflaton zero mode in this case, although the fluctuations will grow and will be responsible for the dynamics.

We can understand the early stages of the dynamics analytically as follows. For very weak coupling and early time we can neglect the backreaction in the mode equations, which in both the large  $N$  and Hartree cases become,

$$\left[ \frac{d^2}{d\tau^2} + 3h \frac{d}{d\tau} + \frac{q^2}{a^2(\tau)} - 1 \right] f_q(\tau) = 0, \quad (4.1)$$

$$f_q(0) = \frac{1}{\sqrt{\omega_q}}; \quad \dot{f}_q(\tau) = -i\sqrt{\omega_q}; \quad \omega_q = \sqrt{q^2 + r^2 - 1}. \quad (4.2)$$

The solutions are of the form,

$$f_q(\tau) = \exp\left[-\frac{3}{2}h\tau\right] \{a(q) J_\nu(z) + b(q) J_{-\nu}(z)\}; \quad z = \frac{q}{h} \exp[-h\tau]; \quad \nu = \sqrt{\frac{1}{h^2} + \frac{9}{4}}, \quad (4.3)$$

where the coefficients  $a(q)$  and  $b(q)$  are determined by the initial conditions:

$$b(q) = -\frac{\pi q}{2h \sin \nu\pi} \left[ \frac{i\omega_q - \frac{3}{2}h}{q} J_\nu\left(\frac{q}{h}\right) - J'_\nu\left(\frac{q}{h}\right) \right], \quad (4.4)$$

$$a(q) = \frac{\pi q}{2h \sin \nu\pi} \left[ \frac{i\omega_q - \frac{3}{2}h}{q} J_{-\nu}\left(\frac{q}{h}\right) - J'_{-\nu}\left(\frac{q}{h}\right) \right]. \quad (4.5)$$

For long times,  $e^{h\tau} \geq q/h$ , these mode functions grow exponentially,

$$f_q(\tau) \simeq b(q) J_{-\nu}(z) \simeq \frac{b(q)}{\Gamma(1-\nu)} \left(\frac{2h}{q}\right)^\nu e^{(\nu-3/2)h\tau}. \quad (4.6)$$

The Bessel functions appearing in the expression for the modes  $f_q(\tau)$  can be approximated by their series expansion,



$$f_q(\tau) = \frac{1}{2} \left[ 1 + \frac{1}{\nu} \left( \frac{3}{2} - \frac{q^2}{4h^2} - i \frac{\omega_q}{h} \right) + \mathcal{O} \left( \frac{1}{\nu^2} \right) \right] e^{(\nu-3/2)h\tau} . \quad (4.7)$$

This is an expansion in powers of  $q^2/(\nu h^2)$  and we conclude that  $g\Sigma(\tau)$  is dominated by the modes with  $q \leq \sqrt{h}$ .

The integral for  $g\Sigma(\tau)$  can be approximated by keeping only the modes  $q \leq f\sqrt{h}$ , where  $f$  is a number of order one, and by neglecting the subtraction term which will cancel the contributions from high momenta. Numerically, even with the backreaction taken into account, the integral is dominated by modes  $q \leq f \approx 10 - 20$  in all of the cases that we studied (see fig. (1.e) below).

The contribution to the fluctuations from these unstable modes is:

$$g\Sigma(\tau) \simeq \sqrt{\frac{\lambda}{6}} \frac{f^3 h^{3/2} r m_R^2}{4\pi^2 M_0^2} \left( 1 + \frac{M_0^2}{m_R^2} \right) e^{(2\nu-3)h\tau} , \quad (4.8)$$

where again, we have taken the high temperature limit,  $T_i \sim T_c \gg m_R$ .

From this equation, we can estimate the value of  $\tau_s$ , the “spinodal time”, at which the contribution of the quantum fluctuations becomes comparable to the contribution from the tree level terms in the equations of motion. This time scale is obtained from the condition  $g\Sigma(\tau_s) = \mathcal{O}(1)$ :

$$\tau_s \simeq -\frac{1}{(2\nu-3)h} \ln \left[ \sqrt{\frac{\lambda}{6}} \frac{f^3 h^{3/2}}{4\pi^2 m_R M_0^2} \frac{T_i}{T_c} \left( 1 + \frac{M_0^2}{m_R^2} \right) \right] , \quad (4.9)$$

which is in good agreement with our numerical results, as will become clear below (see figures (1.a), (2.a) and (3.b)). For values of  $h \geq 1$ , which, as argued below, lead to the most interesting case, an estimate for the spinodal time is,

$$\tau_s \simeq \frac{3h}{2} \ln[1/\sqrt{\lambda}] + \mathcal{O}(1) \quad (4.10)$$

which is consistent with our numerical results (see figure (1.a)).

For  $\tau > \tau_s$ , the effects of backreaction become very important, and the contribution from the quantum fluctuations competes with the tree level terms in the equations of motion, shutting-off the instabilities. Beyond  $\tau_s$ , only a full numerical analysis will capture the correct dynamics.

It is worth mentioning that had we chosen zero temperature initial conditions, then the coupling  $\bar{g} \rightarrow g$  (see (3.20)) and the estimate for the spinodal time would have been,

$$\tau_s \simeq \frac{3h}{2} \ln[1/\lambda] + \mathcal{O}(1), \quad (4.11)$$

that is, roughly a factor 2 larger than the estimate for which the de Sitter stage began at a temperature above the critical value. Therefore (4.10) represents an *underestimate* of the spinodal time scale at which fluctuations become comparable to tree level contributions.

The number of e-folds occurring during the stage of growth of spinodal fluctuations is therefore,

$$\mathcal{N}_e \approx \frac{3h^2}{2} \ln[1/\sqrt{\lambda}], \quad (4.12)$$

or in the zero temperature case,

$$\mathcal{N}_e \approx \frac{3h^2}{2} \ln[1/\lambda], \quad (4.13)$$

which is a factor 2 larger. Thus, it becomes clear that with  $\lambda \approx 10^{-12}$  and  $h \geq 2$ , a required number of e-folds,  $\mathcal{N}_e \approx 100$  can easily be accommodated before the fluctuations become large, modifying the dynamics and the equation of state.

The implications of these estimates are important. The first conclusion drawn from these estimates is that a “quench” approximation is well justified (see figure (1.a)). While the temperature drops from an initial value of a few times the critical temperature to below critical in just a few e-folds, the contribution of the quantum fluctuations needs a large number of e-folds to grow to compensate for the tree-level terms and overcome the instabilities. Only for a strongly coupled theory is the time scale for the quantum fluctuations to grow short enough to restore local thermodynamic equilibrium during the transition.

The second conclusion is that most of the growth of spinodal fluctuations occurs during the inflationary stage, and with  $\lambda \approx 10^{-12}$  and  $H \geq m_R$ , the quantum fluctuations become of the order of the tree-level contributions to the equations of motion within the number of e-folds necessary to solve the horizon and flatness problems. Since the fluctuations grow to become of the order of the tree level contributions at times of the order of this time scale, for larger times they will modify the equation of state substantially and will be shown to provide a graceful exit from the inflationary phase within an acceptable number of e-folds.

For  $\tau < \tau_s$ , when the contribution from the renormalized quantum fluctuations can be ignored, the Hubble constant is given by the classical contribution to the energy density. In terms of the dimensionless quantities introduced above (3.10), we have,

$$H = \frac{16\pi m_R^4}{3\lambda M_{pl}^2} \left[ \frac{\dot{\eta}^2}{2} + \frac{1}{4}(\eta^2 - 1)^2 \right]. \quad (4.14)$$

In the situation we consider here, with  $\dot{\eta} = \eta = 0$ , the condition that  $h \geq 2$  for  $\lambda \simeq 10^{-12}$  translates into  $m_R \simeq 10^{13}$  GeV, which is an acceptable bound on the inflaton mass.

To understand more clearly whether or not the effect of quantum fluctuations and growth of unstable modes during the inflationary phase transition can provide a graceful exit scenario, we must study in detail the contribution to the energy and the equation of state of these quantum fluctuations.

Although we are working in a fixed de Sitter background, the energy and pressure will evolve dynamically. A measure of the backreaction effects of quantum fluctuations on the dynamics of the scale factor is obtained from defining the ‘effective Hubble constant’,

$$\mathcal{H}^2(\tau) = \frac{8\pi}{3M_{pl}^2} \varepsilon(\tau). \quad (4.15)$$

Therefore, the quantities,

$$\frac{\mathcal{H}(\tau)}{\mathcal{H}(0)} = \sqrt{\frac{\varepsilon(\tau)}{\varepsilon(0)}}, \quad (4.16)$$

and

$$\frac{\dot{\mathcal{H}}(\tau)}{\mathcal{H}^2(\tau)} = -\frac{3}{2} \left[ 1 + \frac{p(\tau)}{\varepsilon(\tau)} \right], \quad (4.17)$$

give dynamical information of the effects of the backreaction of the quantum fluctuations on the dynamics of the scale factor. Whenever  $p(\tau) + \varepsilon(\tau) \neq 0$ ,  $\mathcal{H}(\tau)/\mathcal{H}(0) \neq 1$ , or  $\dot{\mathcal{H}}(\tau)/\mathcal{H}^2(\tau) \neq 0$ , the backreaction from the quantum fluctuations will dramatically change the dynamics of the scale factor, and it will no longer be consistent to treat the scale factor as fixed. When  $\mathcal{H}(\tau)/\mathcal{H}(0) \ll 1$  the de Sitter era will end.

From this point onwards only a full treatment of the backreaction, *including* the correct dynamics of the scale factor, will describe the physics. The time scale on which the quantum fluctuations will begin to influence the dynamics of the scale factor is of the order of the spinodal time estimated above, since the contribution of the quantum fluctuations becomes comparable to the tree level terms and modifies the equation of state.

Therefore, there is the possibility that the growth of quantum fluctuations can provide a graceful exit from the inflationary phase, even when the zero mode *does not roll*. The parameters should be chosen in such a way so that the requisite 60 or more e-folds of expansion take place before the spinodal time. From the estimates provided above, this is relatively easy to accommodate with reasonable values of the inflaton mass and for the weak coupling that is usually assumed in inflationary models.

## B. Numerical Analysis

We now solve the large  $N$  set of equations (3.13) numerically, with the initial conditions (3.14), taking  $\dot{\eta}(0) = \eta(0) = 0$ .

The numerical code is based on a fourth order Runge-Kutta algorithm for the differential equation and an 11-points Newton-Cotes algorithm for the integral, with a typical relative errors  $10^{-9}$  in the differential equation and in the integrals. We have tested for cutoff insensitivity with cutoffs  $q_{max} \approx 50 ; 100 ; 150$  with no appreciable variation in the numerical results. The reason for this cutoff insensitivity is due to the fact that only long-wavelength modes grow in amplitude to become non-perturbatively large, whereas the short-wavelength modes always have perturbatively small amplitudes. We have chosen  $r = T_i/T_c = 2$  as a representative value and  $\lambda = 10^{-12}$ . The insensitivity on the value of the cutoff confirms that the high-temperature limit (3.19) is warranted.

As argued previously, for  $\lambda \approx 10^{-12}$ , the cosmologically interesting time scales for the spinodal instabilities to grow during say the first 60-100 e-folds of inflation occur for  $h \geq 1$ , leading to  $H \geq m_R \geq 10^{13}$  GeV which is a phenomenologically acceptable range for the Hubble constant during the inflationary stage.

Figure (1.a) shows the contribution from the quantum fluctuations,  $g\Sigma(\tau)$  vs.  $\tau$  for  $\lambda = 10^{-12}$  ;  $T_i/T_c = 2$  ;  $h = 2$  ;  $\eta(0) = 0$  ;  $\dot{\eta}(0) = 0$ . The quantum fluctuations, as measured by  $g\Sigma(\tau)$ , grow to be of order 1 in a time scale  $\tau \approx 40$  which is the time scale predicted by the early time estimate (4.10). Figure (1.b) shows  $[p(\tau) + \varepsilon(\tau)] \lambda / (2m_R^4)$  vs.  $\tau$  for the same values of figure (1.a). Initially,  $p = -\varepsilon$  and the quantity  $p + \varepsilon$  is zero. At the spinodal time, there is a change in the equation of state, causing  $p + \varepsilon$  to grow. However for late times, the energy density and pressure are each redshifted away such that the sum again approaches zero. We have checked numerically that the energy is covariantly conserved, obeying the relation  $\dot{\varepsilon} + 3H(p + \varepsilon) = 0$  to our numerical accuracy of one part in  $10^7$ . Figures (1.c,d) show  $\mathcal{H}(\tau)/\mathcal{H}(0)$  and  $\dot{\mathcal{H}}(\tau)/\mathcal{H}^2(\tau)$  vs.  $\tau$  respectively. These figures show clearly that when the spinodal quantum fluctuations become comparable to the tree level contribution to the equations of motion, the backreaction on the scale factor becomes fairly large. At this point, the approximation of keeping a fixed background breaks down and the full self-consistent dynamics will have to be studied. At this time, the inflationary stage basically ends since  $\mathcal{H}$  is no longer constant. This occurs for  $\tau \approx 40$  giving about 80 e-folds of inflation during the time in which  $\mathcal{H}$  is approximately constant and equal to  $H$ . Therefore, this new mechanism of spinodal fluctuations, with the zero mode sitting atop the potential hill provides a graceful exit of the inflationary era without any further assumptions

on the evolution of the scalar field.

These fluctuations translate into an amplification of the power spectrum at long wavelengths for  $q \approx h$ . To see this clearly we plot  $g\mathcal{S}(q, \tau)$  with  $\mathcal{S}(q, \tau)$  given by eq. (3.28) vs.  $q$  for  $\tau = 60$  in fig. (1.e). This quantity is very small, because of the coupling constant in front, but for  $\tau \approx \tau_s$  it grows to be of order one for long wavelengths (see also fig. (1.h)) and vanishes very fast for  $q > 10$ . The integral in  $g\Sigma(\tau)$  is dominated by these long wavelengths that become non-perturbatively large, whereas the contribution from the short wavelengths remains always perturbatively small. This is the justification for the approximations performed early that involved only the long-wavelength modes and cutoffs of order  $\sqrt{h}$ . The equal time spatial correlation function given by eq. (3.29) can now be computed explicitly. Figure (1.f) shows  $S(\rho; \tau)/S(0; \tau)$  as a function of  $\rho$  for  $\tau \geq 2$ . We *define* the correlation length  $\xi(\tau)$  as the value of  $\rho$  for which the ratio is  $1/e$ . Figure (1.g) shows  $\xi(\tau)$ ; notice that the correlation length saturates to a value  $\xi(\infty) \approx 1/h$ , and that the correlated regions are of horizon size.

We have performed numerical analysis varying  $h$  with the same values of  $\lambda$  and for the same initial conditions, and found that the only quantitative change is in the time scale for  $g\Sigma(\tau)$  to be of order one. We find that the spinodal time scale grows almost linearly with  $h$  and its numerical value is accurately described by the estimate (4.10). The case in which the Hubble constant is  $h = 0.1$  is shown explicitly. Figure (2.a) shows  $g\Sigma(\tau)$ , which demonstrates the oscillatory behavior similar to what is seen in Minkowski space [26]. The correlation length,  $\xi(\tau)$ , is shown in fig. (2.b); its asymptotic value is again approximately given by  $1/h$ .

### C. The late time limit

For times  $\tau > \tau_s \approx 40$  (for the values of the parameters used in figures (1)) we see from figures (1.a,h) that the dynamics freezes out. The fluctuation,  $g\Sigma(\tau) = 1$ , and the mode functions effectively describe free, minimally coupled, massless particles. The sum rule,

$$-1 + g\Sigma(\infty) = 0, \quad (4.18)$$

is obeyed exactly in the large  $N$  limit as in the Minkowski case [26].

For the Hartree case  $g \rightarrow 3g$ , but the physical phenomena are the same, with the only difference that the sum rule now becomes  $g\Sigma(\infty) = 1/3$ . We now show that this value is a self-consistent solution of the equations of motion for the mode functions, and the *only* stationary solution for asymptotically long times.

In the late time limit, the effective time dependent mass term,  $-1 + \eta^2 + g\Sigma$ , in the equation for the mode functions, (3.13), vanishes (in this case with  $\eta = 0$ ). Therefore, the mode equations (3.13) asymptotically become,

$$\left[ \frac{d^2}{d\tau^2} + 3h \frac{d}{d\tau} + \frac{q^2}{a^2(\tau)} \right] f_q(\tau) = 0 . \quad (4.19)$$

The general solutions are given by,

$$f_q^{asy}(\tau) = \exp \left[ -\frac{3}{2} h \tau \right] \left[ d(q) J_{3/2} \left( \frac{q}{h} e^{-h\tau} \right) + c(q) N_{3/2} \left( \frac{q}{h} e^{-h\tau} \right) \right] , \quad (4.20)$$

where  $J_{3/2}(z)$  and  $N_{3/2}(z)$  are the Bessel and Neumann functions, respectively. The coefficients,  $d(q)$  and  $c(q)$ , can be computed for large  $q$  by matching  $f_q^{asy}(\tau)$  with the WKB approximation to the exact mode functions  $f_q(\tau)$  that obey the initial conditions (3.14). The WKB approximation to  $f_q(\tau)$  has been computed in ref. [25], and we find for large  $q$ ,

$$d(q) = \sqrt{\frac{\pi q}{2h}} \left[ 1 - \frac{i}{q}(h + \Delta) + \mathcal{O}(q^{-2}) \right] e^{-iq/h} + \sqrt{\frac{\pi h}{8q}} \left[ 1 + \mathcal{O}\left(\frac{1}{q}\right) \right] e^{iq/h} , \quad (4.21)$$

$$c(q) = -i\sqrt{\frac{\pi q}{2h}} \left[ 1 - \frac{i}{q}(h + \Delta) + \mathcal{O}(q^{-2}) \right] e^{-iq/h} + i\sqrt{\frac{\pi h}{8q}} \left[ 1 + \mathcal{O}\left(\frac{1}{q}\right) \right] e^{iq/h} , \quad (4.22)$$

where

$$\Delta \equiv \int_0^\infty d\tau e^{h\tau} M^2(\tau) . \quad (4.23)$$

In the  $\tau \rightarrow \infty$  limit, we have for fixed  $q$ ,

$$f_q^{asy}(\tau) \xrightarrow{\tau \rightarrow \infty} -\sqrt{\frac{2}{\pi}} \left( \frac{h}{q} \right)^{3/2} c(q) . \quad (4.24)$$

which are independent of time asymptotically, and explains why the power spectrum of quantum fluctuations freezes at times larger than the spinodal. This behavior is confirmed numerically: fig. (1.h) shows  $\ln [|f_q(\tau)|^2]$  vs.  $\tau$  for  $q = 0, 4, 10$ . Clearly at early times the mode functions grow exponentially, and at times of the order of  $\tau_s$ , when  $g\Sigma(\tau) \approx 1$  the mode functions freeze-out and become independent of time. Notice that the largest  $q$  modes have grown the least, explaining why the integral is dominated by  $q \leq 10 - 20$ .

For asymptotically large times,  $g\Sigma$  is given by,

$$g\Sigma(\infty) = g h^2 \int_0^{+\infty} \frac{dq}{q} \coth \left( \frac{\omega_q}{2\mathcal{T}} \right) \left[ \frac{2h}{\pi} |c(q)|^2 - q \right] , \quad (4.25)$$

where only one term in the UV subtraction survived in the  $\tau = \infty$  limit. For consistency, this integral must converge and be equal to 1 as given by the sum rule. For this to be

the case and to avoid the potential infrared divergence in (4.25), the coefficients  $c(q)$  must vanish at  $q = 0$ . The mode functions are finite in the  $q \rightarrow 0$  limit provided,

$$c(q) \stackrel{q \rightarrow 0}{\simeq} \mathcal{C} q^{3/2} , \quad (4.26)$$

where  $\mathcal{C}$  is a constant.

The numerical analysis and figure (1.e) clearly show that the mode functions remain finite as  $q \rightarrow 0$ , and the coefficient  $\mathcal{C}$  can be read off from these figures. This is a remarkable result. It is well known that for *free* massless minimally coupled fields in de Sitter space-time with Bunch-Davies boundary conditions, the fluctuation contribution  $\langle \psi^2(\vec{x}, t) \rangle$  grows linearly in time as a consequence of the logarithmic divergence in the integrals [12–14]. However, in our case, although the asymptotic mode functions are free, the coefficients that multiply the Bessel functions of order 3/2 have all the information of the interaction and initial conditions and must lead to the consistency of the sum rule. Clearly the sum rule and the initial conditions for the mode functions prevent the coefficients  $d(q)$  and  $c(q)$  from describing the Bunch-Davies vacuum. These coefficients are completely determined by the initial conditions and the dynamics. This is the reason why the fluctuation freezes at long times unlike in the free case in which they grow linearly [12–14].

It is easy to see from eqs.(3.21)-(3.22) and (4.24) that the energy and pressure vanish for  $\tau \rightarrow \infty$ .

Analogously, the two point correlation function can be computed in the late time regime using the asymptotic results obtained above. Inserting eq. (4.20) for the mode functions in eq. (3.29) yields the asymptotic behavior:

$$S(\rho, \tau) \stackrel{\tau \rightarrow \infty}{\simeq} \frac{1}{4\pi^2 \rho} \int_0^\infty q dq \sin q\rho \coth\left(\frac{\omega_q}{2T}\right) \frac{2h^3}{\pi q^3} |c(q)|^2 . \quad (4.27)$$

The asymptotic behavior in time of the equal time correlation function is thus solely a function of  $r$ . The large  $r$  behaviour of  $S(\vec{r}, +\infty)$  is determined by the singularities of  $|c(k)|^2$  in the complex  $k$  plane. We find an exponential decrease,

$$S(\rho, +\infty) \stackrel{\rho \rightarrow \infty}{\simeq} C \frac{e^{-\rho/\xi}}{\rho} , \quad (4.28)$$

where  $\rho = i/\xi$  is the pole nearest to the real axis and  $C$  is some constant. Thus we see that the freeze-out of the mode functions leads to the freeze-out of the correlation length  $\xi$ . The result of the numerical analysis is shown in figs. (1.g) and (2.b) which confirms this behaviour and provides the asymptotic value for  $\xi \approx 1/h$ . From these figures it is also clear that the freeze-out time is given by the expansion time scale,  $1/h$ . More precisely, the

numerical values for  $\xi$  can be accurately reproduced by the following formula obtained by a numerical fit

$$h\xi \simeq 1.02 + 0.2 \ln h + 0.06h + \dots$$

This situation must be contrasted with that in Minkowski space-time [28] where the correlation length grows as  $\xi(\tau) \approx \sqrt{\tau}$  during the stage of spinodal growth. Eventually, this correlation length saturates to a fairly large value that is typically several times larger than the zero temperature correlation length [28]. We see that in the de Sitter case the domains are always horizon-sized.

## V. INFLATON ROLLING DOWN

We now study the situation in which the inflaton zero mode rolls down the potential hill and consider initial conditions such that  $\eta(0) \neq 0$ ;  $\dot{\eta}(0) = 0$ . In this case there will be two competing effects. One will be the growth of spinodal fluctuations analyzed in the previous section, while the other will be the rolling of the zero mode. Which effect will dominate the dynamics is a matter of time scales. Before embarking on a numerical analysis of these cases, it is illuminating to try to understand under what conditions the dynamics will be driven by either the zero mode or the spinodal fluctuations. We will analyze first the case of the large  $N$  equations, and compare later to the Hartree case.

The large  $N$  equations are summarized by equations (3.12) - (3.14). The important part of the mode equations that determine the spinodal growth of long-wavelength modes is the term,  $\eta^2 + g\Sigma$ . We can obtain an approximate estimate for the time scales on which the contribution of the zero mode becomes significant as follows. Let us consider the situation in which  $\eta(0) \ll 1$  and neglect the non-linear and backreaction terms (the last two terms) in the equation of motion for the zero mode (3.12). At long times, but smaller than the time at which either the quantum fluctuation or  $\eta$  become of  $\mathcal{O}(1)$ , we find,

$$\eta(\tau) \approx \eta(0)e^{(\nu-3/2)h\tau}, \quad (5.1)$$

with  $\nu$  given in eqn.(4.3). The estimate for the time scale for the zero mode to be,  $\eta_f \approx \mathcal{O}(1)$ , is approximately given by,

$$\tau_{zm} \approx \frac{2}{(2\nu-3)h} \ln \left[ \frac{\eta_f}{\eta(0)} \right]. \quad (5.2)$$

Comparing this time scale to the spinodal time scale given by (4.10), for which quantum fluctuations grow to be of  $\mathcal{O}(1)$ , we see that when,



$$\eta(0) \ll \lambda^{1/4}, \quad (5.3)$$

the quantum fluctuations will grow to be  $\mathcal{O}(1)$  much *earlier* than the zero mode for  $T_i > T_c$  (for  $T_i = 0$  the bound becomes  $\eta(0) \ll \lambda^{1/2}$ ). In this case the dynamics will be driven completely by the quantum fluctuations, as the zero mode will be rolling down the potential hill very slowly and will not grow enough to compete with the quantum fluctuations before the fluctuations grow to overcome the tree level terms in the equations of motion. In this case, as argued previously, the large  $N$  and Hartree approximations will be completely equivalent during the time scales of interest.

On the other hand, if

$$\eta(0) \gg \lambda^{1/4}, \quad (5.4)$$

then the zero mode will roll and become  $\mathcal{O}(1)$  *before* the fluctuations have enough time to grow to  $\mathcal{O}(1)$  ( $\eta(0) \gg \lambda^{1/2}$  for  $T_i = 0$ ). In this case, the dynamics will be dominated by the rolling of the zero mode and is mostly *classical*. The quantum fluctuations remain perturbatively small throughout the inflationary stage which will end when the velocity of the zero mode modifies the equation of state to terminate de Sitter expansion.

For  $\eta(0) \approx \lambda^{1/4}$  (or  $\eta(0) \approx \lambda^{1/2}$  for  $T_i = 0$ ), both the rolling of the zero mode *and* the quantum fluctuations will give contributions of the same order to the dynamics. In this case, the quantum fluctuations will be large for the long-wavelength modes and the classical approximation to the inflationary dynamics will not be accurate.

Since the scenario in which  $\eta(0) \gg \lambda^{1/4}$ , in which the dynamics is basically driven by the classical evolution of the zero mode has received a great deal of attention in the literature, we will *not* focus on this case, but instead analyze numerically the cases in which  $\eta(0) \neq 0$  but such that  $\eta(0) \leq \lambda^{1/4}$ .

### A. Numerical Analysis:

We have evolved the set of equations of motion given by (3.12) and (3.13) numerically with initial conditions (3.14) for the large  $N$  case, and (3.15) and (3.16), with the corresponding initial conditions (3.17) on the mode functions for the Hartree case. The numerical code is the same as in the previous section with the same relative errors.

#### Large $N$ :

Fig. (3.a,b) show  $\eta(\tau)$  and  $g\Sigma(\tau)$  vs.  $\tau$  for the values  $\lambda = 10^{-12}$ ;  $T_i/T_c = 2$ ;  $\eta(0) = 10^{-5}$ ;  $\dot{\eta}(0) = 0$ . Clearly the dynamics is dominated by the fluctuations; the zero mode

grows but is always negligibly small compared to  $g\Sigma(\tau)$ . The time scale at which  $g\Sigma(\tau)$  grows to be of order one is about the same as in the case,  $\eta(0) = 0$ , and all the behavior for the mode functions, correlation length, energy density, pressure, etc. is similar to the case analyzed in the previous section.

Asymptotically, we find that the sum rule,

$$-1 + \eta^2(\infty) + g\Sigma(\infty) = 0, \quad (5.5)$$

is satisfied to our numerical accuracy. This is the same as the situation in Minkowski space-time [25,26], and when  $\eta \neq 0$ , this sum rule is nothing but the Ward identity associated with Goldstone's theorem. The fluctuations are Goldstone bosons, minimally coupled, and the symmetry is spontaneously broken with a very small expectation value for the order parameter as can be read off from figure (3.a). For  $\tau > \tau_s$ , the dynamics freezes completely and the zero mode and the fluctuations achieve their asymptotic values much in the same way as in the case  $\eta = 0$  studied in the previous section. Again, the correlation length becomes independent of time with  $\xi(\infty) \approx 1/h$  in a time scale given by  $1/h$ .

Because there is a damping term in the zero mode equation, it is reasonable to assume that asymptotically there will be a solution with a constant value of  $\eta$ . Then the Ward-identity,  $\eta(\infty)[-1 + \eta^2(\infty) + g\Sigma(\infty)] = 0$ , must be fulfilled. In the large  $N$  case, the *only* stationary solutions are i)  $\eta = 0$ ;  $g\Sigma(\infty) = 1$ , or, ii)  $\eta(\infty) \neq 0$ ;  $-1 + \eta^2(\infty) + g\Sigma(\infty) = 0$ . To have a consistent solution of the mode functions, it must be that the effective mass term  $[-1 + \eta^2(\infty) + g\Sigma(\infty)]$  vanishes asymptotically, leading to the mode equations for massless, minimally coupled modes which are asymptotically independent of time as shown in the previous section (see eq.(4.24)). Furthermore, from fig. (3.b) it is clear that  $g\Sigma(\tau)$  remains constant at long times, again unlike the case of free massless fields with Bunch-Davies boundary conditions in which case the fluctuation grows linearly in time [12–14].

### **Hartree :**

Figure (3.a) also shows the evolution of the zero mode in the large  $N$  and Hartree case. Although there is a quantitative difference in the amplitude of the zero mode, in both cases it is extremely small and gives a negligible contribution to the dynamics. In the Hartree case, however, there is no equivalent of the large  $N$  sum rule; the *only* stationary solution for  $\eta \neq 0$  is,  $\eta^2(\infty) = 1$ ;  $g\Sigma(\infty) = 0$ . Such a solution leads to mode equations with a *positive* mass term and mode functions that vanish exponentially fast for  $\tau \rightarrow \infty$  for all momenta. However, whether the asymptotic behavior of the Hartree solution is achieved within the interesting time scales is a matter of initial conditions. For example in fig. (3.a) the initial condition is such that the time scale for growth of the quantum fluctuations is

much shorter than the time scale for which the amplitude of the zero mode grows large and the non-linearities become important. In the large  $N$  case the sum rule is satisfied with a large value of the quantum fluctuations. In the Hartree case the equivalent sum rule  $-1 + 3\eta_H^2 + 3g\Sigma_H = 0$  is satisfied for a very small  $\eta_H$  and a  $g\Sigma_H \approx 1/3$ . The modes become effectively massless and they stop growing.

The equation for the zero mode (see eqn. (3.15)) still has an uncanceled piece of the non-linearity,  $-2\eta^2$ ; however the derivatives and the amplitude of  $\eta$  are all extremely small and though the zero mode still evolves in time, it does so extremely slowly. In fact the Hartree curve in fig. (3.a) has an extremely small positive slope asymptotically, and while  $\eta_H$  grows very slowly,  $g\Sigma_H$  diminishes at the same rate. In the case shown in fig. (3.a), we find numerically that  $\dot{\eta}_H/\eta_H \approx 10^{-7}$  at  $\tau = 150$ . Before this time most of the interesting dynamics that can be captured with a fixed de Sitter background had already taken place, and the backreaction of the fluctuations on the metric becomes substantial requiring an analysis that treats the scale factor dynamically.

The conclusion of our analysis is that in the region of initial conditions for which the quantum fluctuations dominate the dynamics, that is for  $\eta(0) \ll \lambda^{1/4}$ , both large  $N$  and Hartree give the same answer on the relevant time scales. The figures for  $\mathcal{H}(\tau)/\mathcal{H}(0)$  are numerically indistinguishable from the case of figures (1).

For comparison, we show in figure (4) both cases for the zero mode, for the same values of the parameters as in figures (1,3) but with the initial condition  $\eta(0) = 10^{-3}$  ;  $\dot{\eta}(0) = 0$ . This is a borderline case in which the time scales for the evolution of the zero mode and quantum fluctuations are of the same order and there is no clear separation of time scales between these two competing terms in the evolution equations.

We see that in the large  $N$  case the zero mode rolls to a final amplitude which is  $\mathcal{O}(1)$  and of the same order as  $g\Sigma(\infty)$  and the sum rule is satisfied. However, the Hartree case clearly shows the asymptotics analyzed above with  $\eta_H(\infty) = 1$ ;  $g\Sigma_H(\infty) = 0$ .

This particular borderline case is certainly not generic and would imply some fine tuning of initial conditions. Finally the case in which  $\eta(0) \gg \lambda^{1/4}$  (or  $\lambda^{1/2}$  for  $T_i = 0$ ) is basically classical in that the dynamics is completely given by the classical rolling of the zero mode and the fluctuations are always perturbatively small.

## VI. DISCUSSION AND CONCLUSIONS

We have identified analytically and numerically two distinct regimes for the dynamics determined by the initial condition on the expectation value of the zero mode of the inflaton.

1. When  $\eta(0) \ll \lambda^{1/4}$  (or  $\lambda^{1/2}$  for  $T_i = 0$ ), the dynamics is driven by quantum (and thermal) fluctuations. Spinodal instabilities grow and eventually compete with tree level terms at a time scale,  $\tau_s \geq -3h \ln[\lambda]/2$ . The growth of spinodal fluctuations translates into the growth of spatially correlated domains which attain a maximum correlation length (domain size) of the order of the horizon. For very weak coupling and  $h \geq 1$  this time scale can easily accomodate enough e-folds for inflation to solve the flatness and horizon problems. The quantum fluctuations modify the equation of state dramatically and at this time scale can modify the dynamics of the scale factor and provide a means for a graceful exit to the inflationary stage without slow-roll.

This non-perturbative description of the non-equilibrium effects in this regime in which quantum (and thermal) fluctuations are most important is borne out by both the large N and Hartree approximations. Thus our analysis provides a reliable understanding of the relevant non-perturbative, non-equilibrium effects of the fluctuations that have not been revealed before in this setting.

These initial conditions are rather natural if the de Sitter era arises during a phase transition from a radiation dominated high temperature phase in local thermodynamic equilibrium, in which the order parameter and its time derivative vanish.

2. When  $\eta(0) \gg \lambda^{1/4}$  (or  $\lambda^{1/2}$  for  $T_i = 0$ ), the dynamics is driven solely by the classical evolution of the inflaton zero mode. The quantum and thermal fluctuations are always perturbatively small (after renormalization), and their contribution to the dynamics is negligible for weak couplings. The de Sitter era will end when the kinetic contribution to the energy becomes of the same order as the ‘vacuum’ term. This is the realm of the slow-roll analysis whose characteristics and consequences have been analyzed in the literature at length. These initial conditions, however, necessarily imply some initial state either with a biasing field that favors a non-zero initial expectation value, or that in the radiation dominated stage, prior to the phase transition, the state was strongly out of equilibrium with an expectation value of the zero mode different from zero. Although such a state cannot be ruled out and would naturally arise in chaotic scenarios, the description of the phase transition in this case requires further input on the nature of the state prior to the phase transition.

We have learned from this work that non-equilibrium effects can alter scalar field dynamics in a dramatic way, under well specified and physically reasonable conditions. In particular, this results bring up the tantalizing possibility that when the scale factor is

coupled to the inflaton dynamically, in a full backreaction treatment, some of the standard results concerning the time evolution of the inflaton could be modified in unexpected ways. The fact that we found massless fields whose fluctuations did *not* grow linearly is an extremely interesting result, especially in light of how the quantum fluctuations become density perturbations. We are currently working on the formalism that allows us to couple gravity dynamically in a non-equilibrium way. Furthermore, it would be interesting to extend the program of reconstruction of the inflaton effective potential (see [35]) to include the possibility of the dynamics being driven by spinodal fluctuations and not by “slow roll” of the inflaton zero mode.

The results presented here raise some further interesting questions: how do these fluctuations contribute to the spectrum of primordial scalar density perturbations? How should the approach to cosmological perturbations based on slow-roll be modified to the case studied here in which spinodal fluctuations, *not* slow-roll drive the dynamics? We are currently studying these issues within the consistent non-perturbative, non-equilibrium program presented in this article.

## ACKNOWLEDGMENTS

D. B. would like to thank the N.S.F for partial support through the grant awards: PHY-9302534 and INT-9216755, the Pittsburgh Supercomputer Center for grant award No: PHY950011P and LPTHE for warm hospitality. R. H. and D. C. were supported by DOE grant DE-FG02-91-ER40682.

## REFERENCES

- [1] A. H. Guth, Phys. Rev. D 23, 347 (1981).
- [2] A. H. Guth and E. J. Weinberg, Nucl. Phys. B212, 321 (1983); S. W. Hawking, I. Moss and J. Stewart, Phys. Rev. D26, 2681 (1982).
- [3] A. D. Linde, Phys. Lett. 108B, 389 (1982).
- [4] A. Albrecht and P. J. Steinhardt, Phys. Rev. Lett. 48, 1220 (1982).
- [5] A. D. Linde, Phys. Lett. 129B, 177 (1983).
- [6] For reviews of inflationary cosmology, see R. H. Brandenberger, Rev. of Mod. Phys. 57, 1 (1985); Int. J. Mod. Phys. A2, 77 (1987).
- [7] L. Abbott and S-Y. Pi, Inflationary Cosmology, World Scientific, 1986.
- [8] E. W. Kolb and M. S. Turner, The Early Universe (Addison Wesley, Redwood City, 1990).
- [9] A. Linde, Particle Physics and Inflationary Cosmology, (Harwood Academic Publishers, Switzerland, 1990); For a recent summary of inflationary cosmology see: A. Linde: “Lectures on Inflationary Cosmology”, in Current Topics in Astrofundamental Physics, ‘The Early Universe’, Proceedings of the Chalonge Erice School, N. Sánchez and A. Zichichi Editors, Nato ASI series C, vol. 467, 1995, Kluwer Acad. Publ.; L. Kofman, gr-qc/9508019 (1996).
- [10] For reviews on topological defects in early universe cosmology, see: A. Vilenkin and E. P.S. Shellard, Cosmic Strings and other Topological Defects (Cambridge University Press, 1994); M. B. Hindmarsh and T. W. B. Kibble, Rep. Prog. Phys. 58, 477 (1995).
- [11] A. Vilenkin, Phys. Lett. B115, 91 (1982).
- [12] A.D. Linde, Phys. Lett. B116, 335 (1982).
- [13] A. Vilenkin and L. H. Ford, Phys. Rev. D26, 1231 (1982).
- [14] A. Vilenkin, Nucl. Phys. B226, 504 (1983); Nucl. Phys. B226, 527 (1986).
- [15] G. F. Mazenko, W. G. Unruh and R. M. Wald, Phys. Rev. D31, 273 (1985); G. F. Mazenko, Phys. Rev. Lett. 54, 2163 (1985).
- [16] A. Guth and S-Y. Pi, Phys. Rev. **D32**, 1899 (1985).

- [17] For a thorough exposition of non-equilibrium methods in cosmology see, for example: E. Calzetta and B. L. Hu, Phys. Rev. D35, 495 (1988); *ibid* D37, 2838 (1988); J. P. Paz, Phys. Rev. D41, 1054 (1990); *ibid* D42, 529 (1990); B. L. Hu, Lectures given at the Canadian Summer School For Theoretical Physics and the Third International Workshop on Thermal Field Theories (Banff, Canada, 1993) (to appear in the proceedings) and in the Proceedings of the Second Paris Cosmology Colloquium, Observatoire de Paris, June 1994, p.111, H. J. de Vega and N. Sánchez Editors, World Scientific, 1995, and references therein.
- [18] A. Ringwald, Ann. of Phys. (N.Y.) 177, 129 (1987); Phys. Rev. D 36, 2598 (1987).
- [19] H. Leutwyler and S. Mallik, Ann. of Phys. (N.Y.) 205, 1 (1991).
- [20] G. Semenoff and N. Weiss, Phys. Rev. D31; 699 (1985).
- [21] For non-equilibrium methods in different contexts see for example: F. Cooper, J. M. Eisenberg, Y. Kluger, E. Mottola, B. Svetitsky, Phys. Rev. Lett. 67, 2427 (1991); F. Cooper, J. M. Eisenberg, Y. Kluger, E. Mottola, B. Svetitsky, Phys. Rev. D48, 190 (1993).
- [22] F. Cooper and E. Mottola, Mod. Phys. Lett. A 2, 635 (1987); F. Cooper, S. Habib, Y. Kluger, E. Mottola, J. P. Paz, P. R. Anderson, Phys. Rev. D50, 2848 (1994). F. Cooper, S.-Y. Pi and P. N. Stancioff, Phys. Rev. D34, 3831 (1986). F. Cooper, Y. Kluger, E. Mottola, J. P. Paz, Phys. Rev. D51, 2377 (1995). F. Cooper and E. Mottola, Phys. Rev. D36, 3114 (1987).
- [23] O. Eboli, R. Jackiw and S-Y. Pi, Phys. Rev. D37, 3557 (1988); M.Samiullah, O. Eboli and S-Y. Pi, Phys. Rev. D44, 2335 (1991).
- [24] J. Guven, B. Liebermann and C. Hill, Phys. Rev. D39, 438 (1989).
- [25] D. Boyanovsky, H. J. de Vega, and R. Holman, Phys. Rev. **D49**, 2769 (1994).
- [26] D. Boyanovsky, H. J. de Vega, R. Holman, D.-S. Lee and A. Singh, Phys. Rev. **D51**, 4419 (1995); D. Boyanovsky, M. D’Attanasio, H. J. de Vega, R. Holman and D. S. Lee, Phys. Rev. **D52**, 6805 (1995); D. Boyanovsky, M. D’Attanasio, H. J. de Vega and R. Holman, Phys. Rev. **D54**, 1748 (1996). D. Boyanovsky, H. J. de Vega, R. Holman and J. Salgado, ‘Analytic and Numerical Study of Reheating Dynamics’ (to appear in Phys. Rev.D Dic 1996), hep-ph/9608205). D. Boyanovsky, D. Cormier, H. J. de Vega, R. Holman, A. Singh and M. Srednicki, ‘Preheating in FRW Universes’ (submitted to

- P.R.L. 1996, hep-ph/9609527). For reviews see, D. Boyanovsky, H. J. de Vega and R. Holman, in the Proceedings of the Second Paris Cosmology Colloquium, Observatoire de Paris, June 1994, p. 127-215, H. J. de Vega and N. Sánchez Editors, World Scientific, 1995; D. Boyanovsky, M. D’Attanasio, H. J. de Vega, R. Holman and D.-S. Lee, ‘New aspects of reheating’, in the Proceedings of the Erice Chalonge School, ‘String Gravity and Physics at the Planck Energy Scale’, NATO Advanced Study Institute, N. Sánchez and A. Zichichi Editors, Kluwer 1996, p. 451-492.
- [27] D. Boyanovsky and H. J. de Vega, Phys. Rev. **D47**, 2343 (1993).
  - [28] D. Boyanovsky, D-S. Lee, and A. Singh, Phys. Rev. **D48**, 800 (1993).
  - [29] F. Cooper, S. Habib, Y. Kluger and E. Mottola, “Non-Equilibrium dynamics of symmetry breaking in  $\Phi^4$  field theory”, (hep-ph/9610345).
  - [30] F. Cooper and E. Mottola, Mod. Phys. Lett. A2, 635 (1987).
  - [31] T. S. Bunch and P.C.W. Davies, Proc. R. Soc. London A360,117 (1978); see also ref. [32].
  - [32] N. D. Birrell and P.C.W. Davies, “Quantum fields in curved space” Cambridge Univ. Press, (Cambridge, 1986).
  - [33] P. R. Anderson, Phys. Rev. **D32**, 1302 (1985).
  - [34] A. P. Prudnikov, Yu. A. Brichkov and O. I. Marichev, Integrals and Series, vol. 2, Ed. Nauka, Moscow, 1983.
  - [35] See for example the recent review by J. E. Lidsey, A. R. Liddle, E. W. Kolb, E. J. Copeland, T. Barreiro and M. Abney: “Reconstructing the Inflaton Potential-an overview” (Fermilab Pub 95-280-A; astro-ph/9508078, 1995).



### Figure Captions:

**Fig. 1a:**  $g\Sigma(\tau)$  vs.  $\tau$  for  $\eta(0) = \dot{\eta}(0) = 0$ ;  $\lambda = 10^{-12}$ ;  $r = 2$ ;  $h = 2$ .

**Fig. 1b:**  $\lambda[p(\tau) + \varepsilon(\tau)]/2m_r^4$  vs.  $\tau$  for the same values of parameters as in fig. 1a.

**Fig. 1c:**  $\mathcal{H}(\tau)/\mathcal{H}(0)$  vs  $\tau$  for the same parameters as in fig. 1a.

**Fig. 1d:**  $\dot{\mathcal{H}}(\tau)/\mathcal{H}^2(\tau)$  vs  $\tau$  for the same values as in fig. 1a.

**Fig. 1e:**  $g\mathcal{S}(q, \tau)$  vs.  $q$  for  $\tau = 60$ . Same parameters as in fig. 1a.

**Fig. 1f:**  $S(\rho, \tau)/S(0, \tau)$  vs.  $\rho$  for  $\tau \geq 2$ . Same parameters as in fig. 1a.

**Fig. 1g:**  $\xi(\tau)$  vs  $\tau$ . Same parameters as in fig. 1a.

**Fig. 1h:**  $\ln[|f_q(\tau)|^2]$  vs.  $\tau$  for  $q = 0, 4, 10$ . Same parameters as in fig. 1a.

**Fig. 2a:**  $g\Sigma(\tau)$  vs.  $\tau$  for  $\eta(0) = \dot{\eta}(0) = 0$ ;  $\lambda = 10^{-12}$ ;  $r = 2$ ;  $h = 0.1$ .

**Fig. 2b:**  $\xi(\tau)$  vs  $\tau$ . Same parameters as in fig. 2a.

**Fig. 3a:**  $\eta(\tau)$  vs.  $\tau$  for  $\lambda = 10^{-12}$ ;  $r = 2$ ;  $h = 2$ ;  $\eta(0) = 10^{-5}$ ;  $\dot{\eta}(0) = 0$  for large  $N$  (solid curve) and Hartree (dashed curve).

**Fig. 3b:**  $g\Sigma(\tau)$  vs.  $\tau$  for the same values of the parameters as in fig. 3a, for large  $N$  (solid curve) and Hartree (dashed curve).

**Fig. 4:** Comparison of zero mode dynamics for large  $N$  (solid curve) and Hartree (dashed curve) for  $\eta(0) = 10^{-3}$ ;  $\dot{\eta}(0) = 0$  and all other parameters as in figures (1,2).

Figure 1a

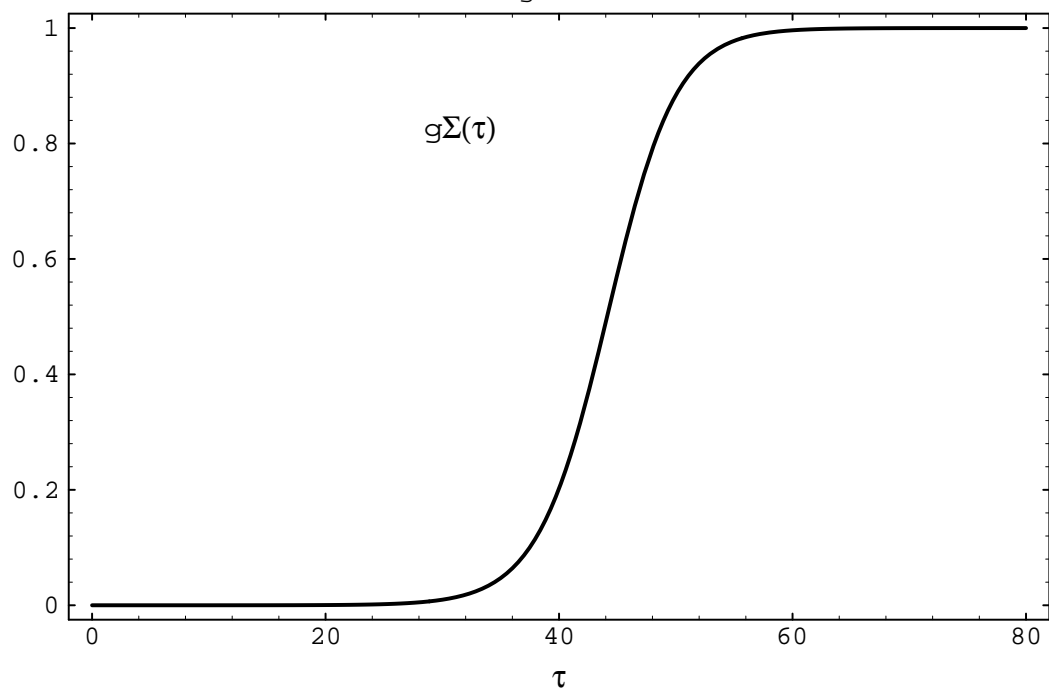


Figure 1b

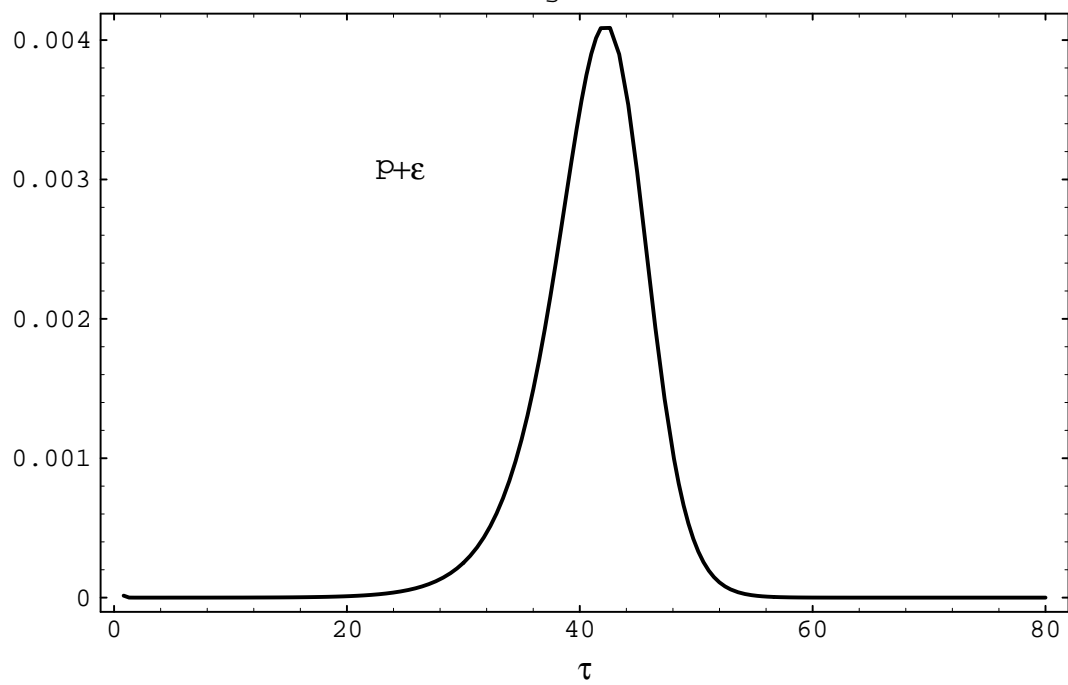


Figure 1c

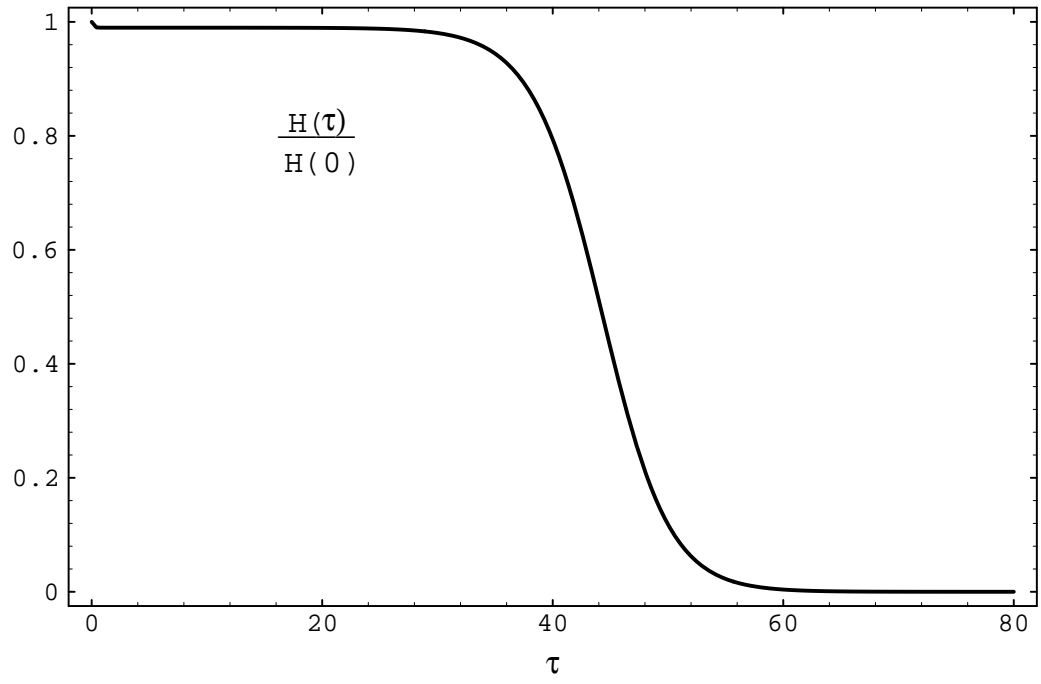


Figure 1d

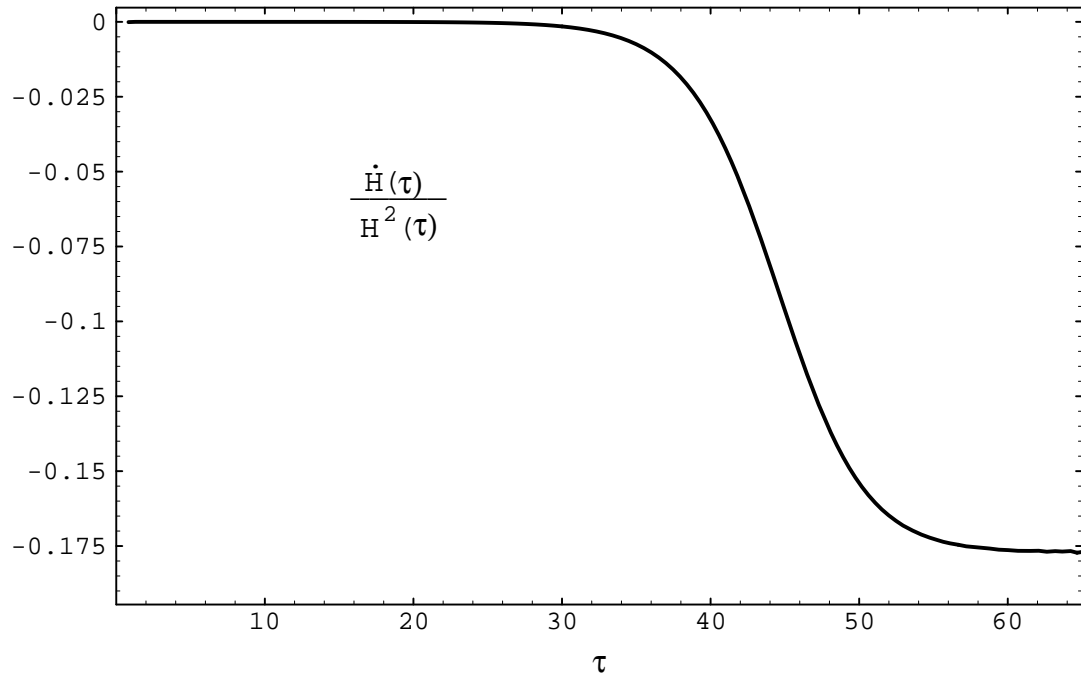


Figure 1e

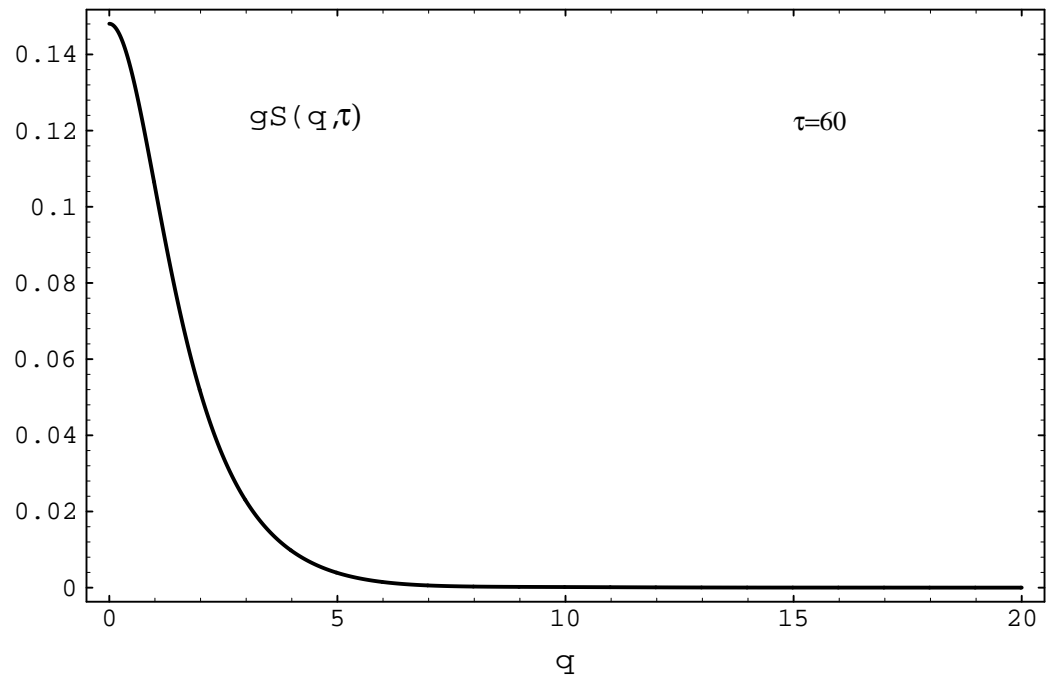


Figure 1f

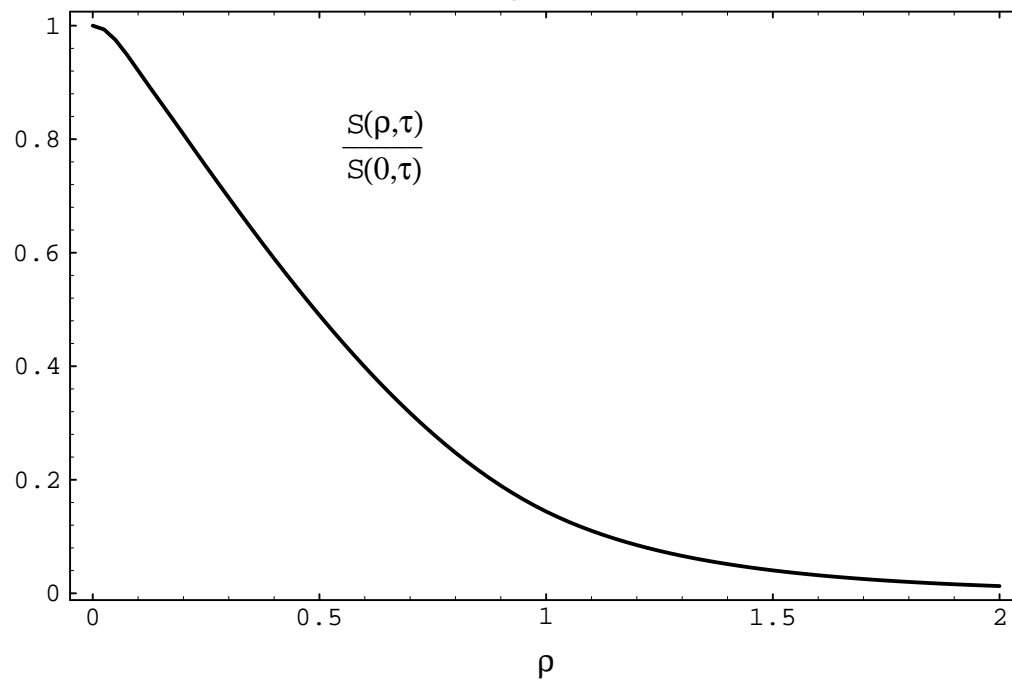


Figure 1g

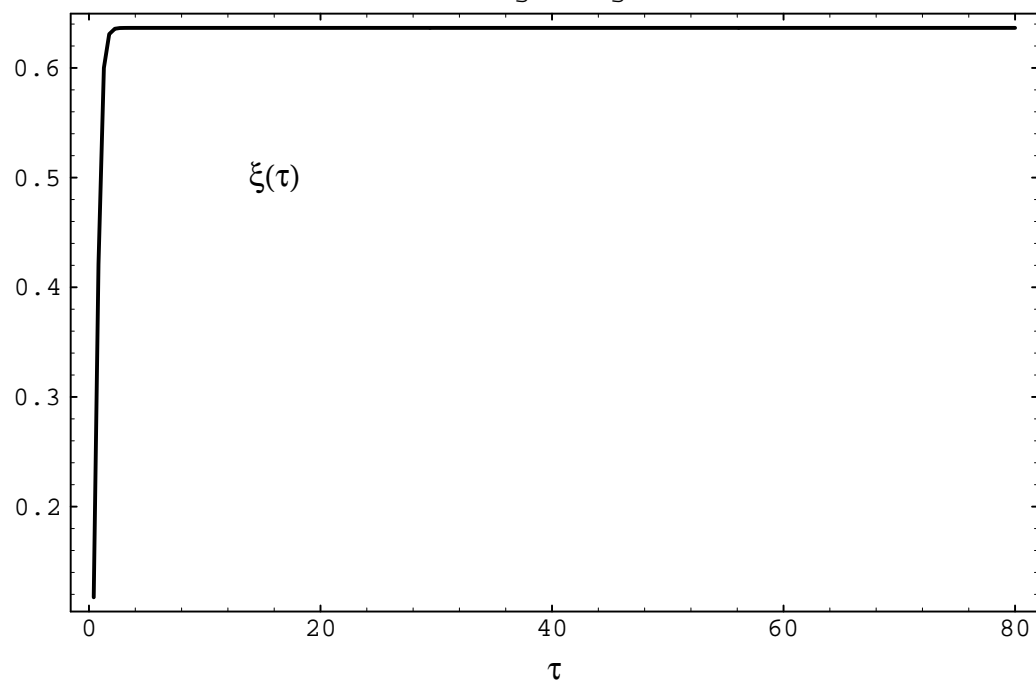




Figure 1h

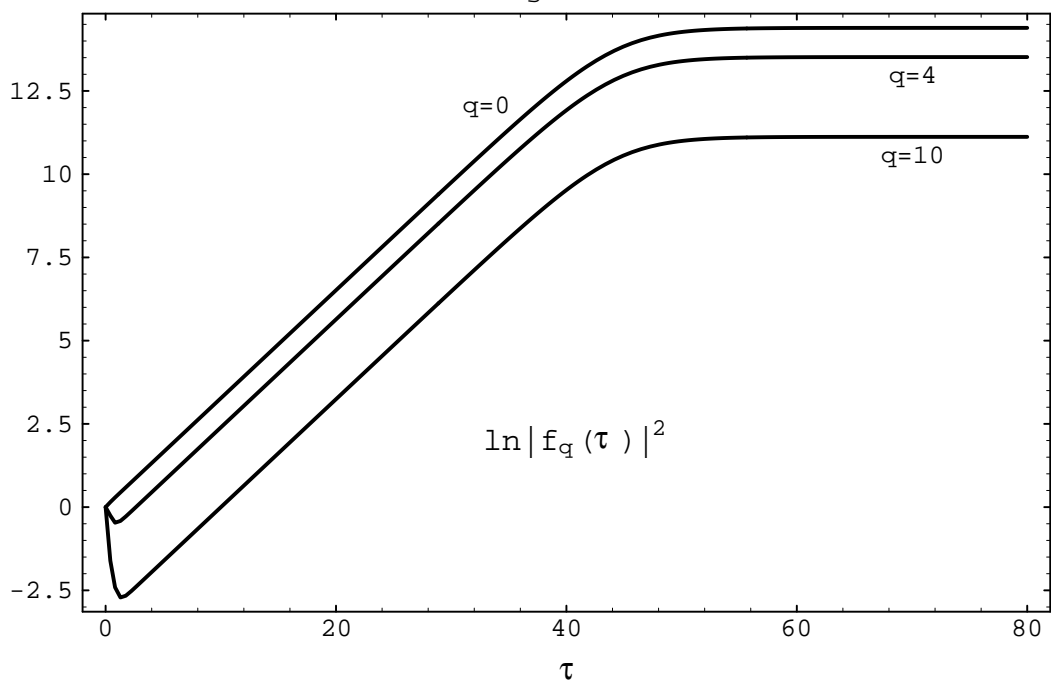


Figure 2a

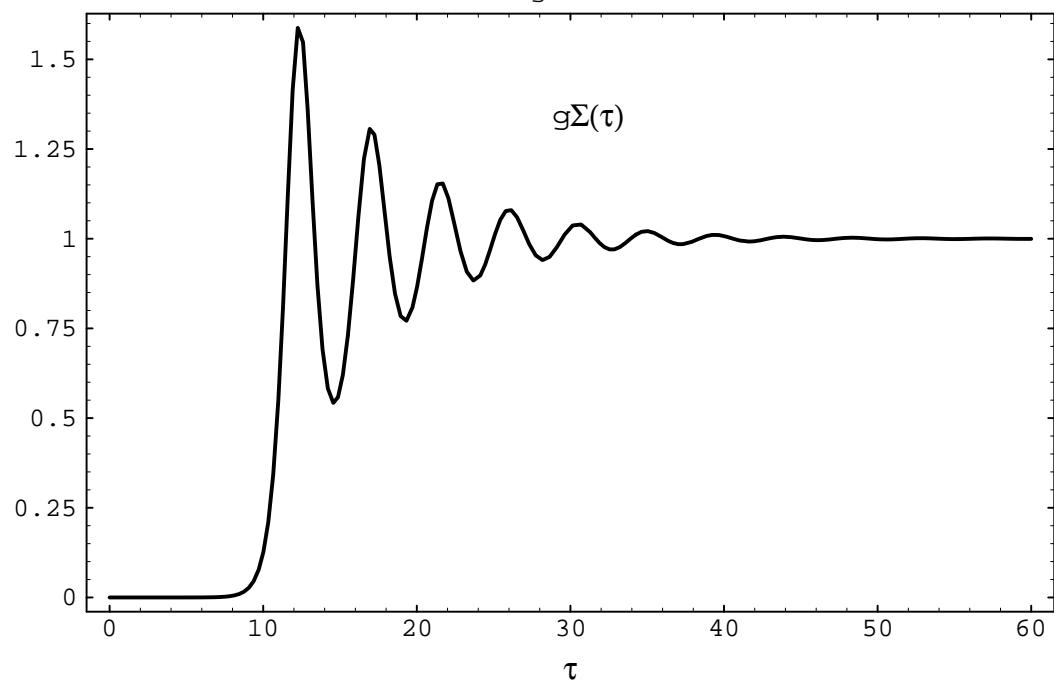


Figure 2b

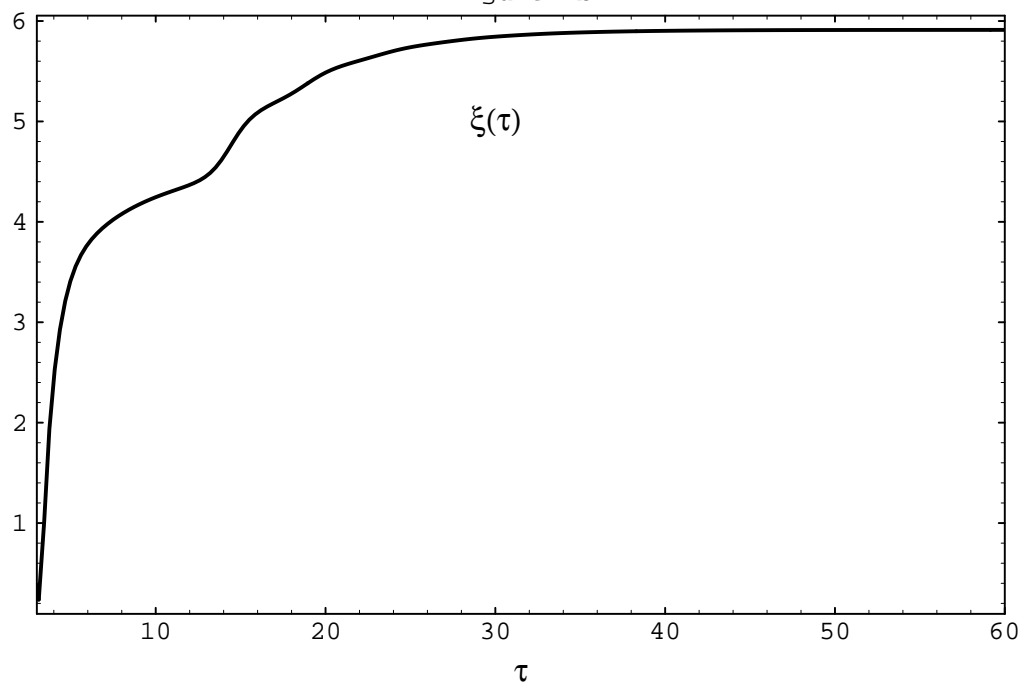


Figure 3a

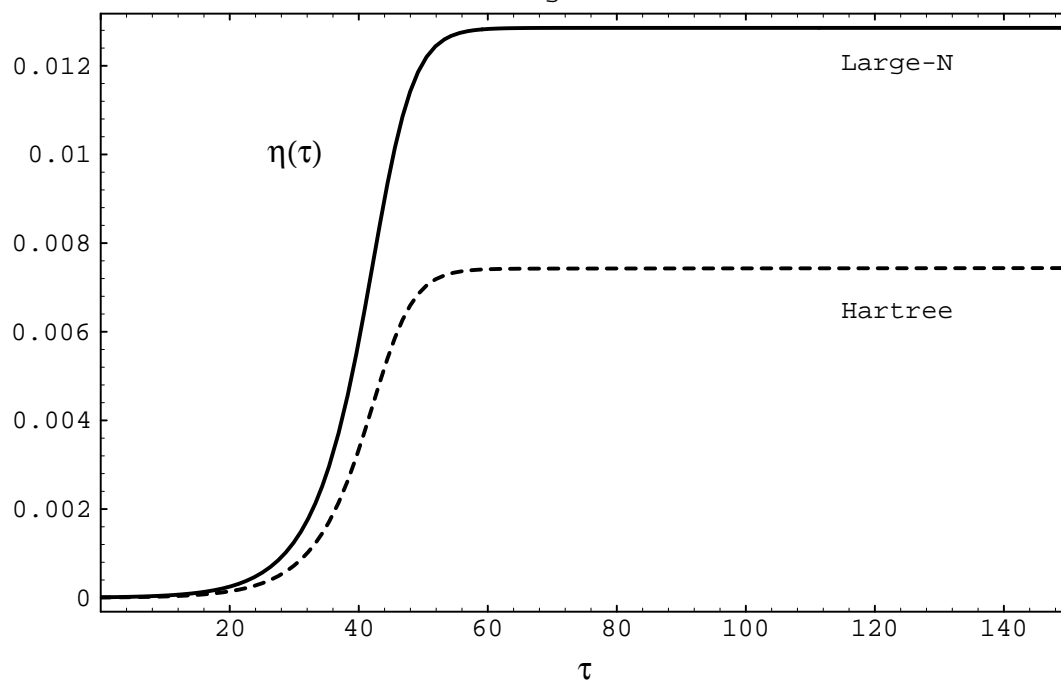


Figure 3b

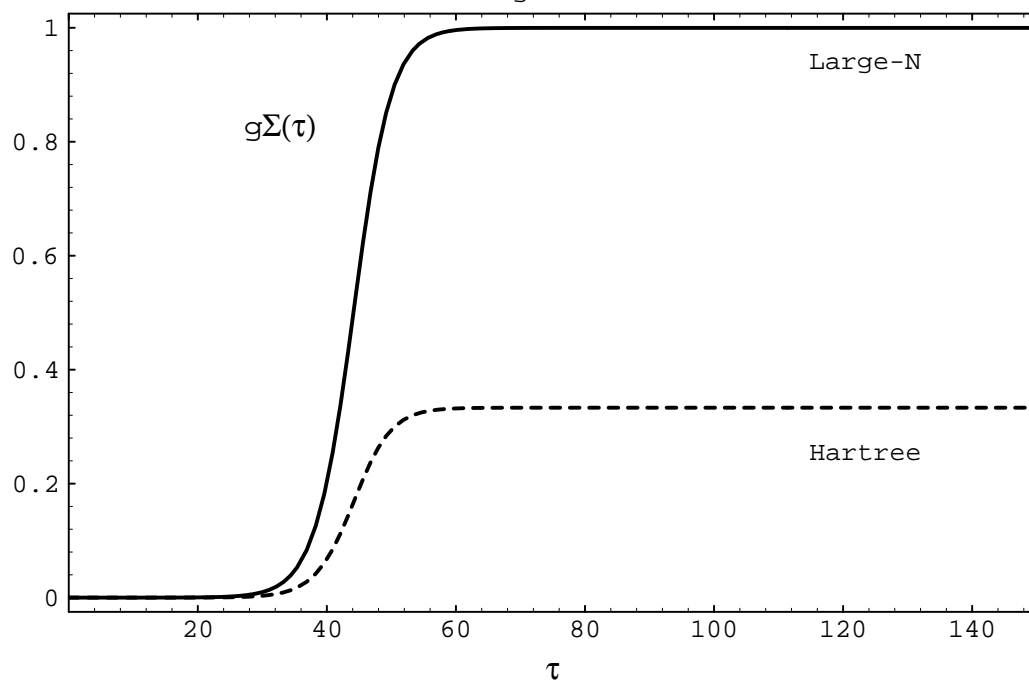


Figure 4

